N^6-Cycloalkyl- and N^6-Bicycloalkyl-*C*5′(*C*2′)-modified Adenosine Derivatives as High-Affinity and Selective Agonists at the Human A_1 Adenosine Receptor with Antinociceptive Effects in Mice

Palmarisa Franchetti,[†] Loredana Cappellacci,[†] Patrizia Vita,[†] Riccardo Petrelli,[†] Antonio Lavecchia,[‡] Sonja Kachler,[§] Karl-Norbert Klotz,[§] Ida Marabese,[∥] Livio Luongo,[∥] Sabatino Maione,[∥] and Mario Grifantini*[,†]

Department of Chemical Sciences, University of Camerino, 62032 Camerino, Italy, Department of Pharmaceutical and Toxicological Chemistry, University of Naples "Federico II", 80131 Naples, Italy, Institut für Pharmakologie and Toxikologie, Universität Würzburg, D-97078 Würzburg, Germany, and Department of Experimental Medicine, Section of Pharmacology L. Donatelli, Second University of Naples, 80138 Naples, Italy

Received November 18, 2008

To further investigate new potent and selective human A_1 adenosine receptor agonists, we have synthesized a series of 5′-chloro-5′-deoxy- and 5′-(2-fluorophenylthio)-5′-deoxy-N^6-cycloalkyl(bicycloalkyl)-substituted adenosine and 2′-*C*-methyladenosine derivatives. These compounds were evaluated for affinity and efficacy at human A_1, A_{2A}, A_{2B}, and A_3 adenosine receptors. In the series of N^6-cyclopentyl- and N^6-(*endo*-norborn-2-yl)adenosine derivatives, 5′-chloro-5′-deoxy-CPA (**1**) and 5′-chloro-5′-deoxy-(±)-ENBA (**3**) displayed the highest affinity in the subnanomolar range and relevant selectivity for hA_1 vs the other human receptor subtypes. The higher affinity and selectivity of 5′-chloro-5′-deoxyribonucleoside derivatives **1** and **3** for hA_1 AR vs hA_3 AR compared to that of the parent 5′-hydroxy compounds CPA and (±)-ENBA was rationalized by a molecular modeling analysis. 5′-Chloro-5′-deoxy-(±)-ENBA, evaluated for analgesic activity in the formalin test in mice, was found to inhibit the first or the second phases of the nocifensive response induced by intrapaw injection of formalin at doses ranging between 1 and 2 mg/kg i.p.

Introduction

Adenosine mediates a wide variety of physiological effects by activation of four G protein-coupled receptors (A_1, A_{2A}, A_{2B}, and A_3 ARs) that are widely distributed throughout the body. A number of agonists with high affinity for human A_1, A_{2A}, and A_3 adenosine receptors and more recently for the A_{2B} subtype have been developed for therapeutic applications, and some are in clinical trials for various conditions.[1] Effects mediated by the selective activation of A_1 AR include neuro- and cardioprotection, an antiarrhythmic effect, reduction of neuropathic pain, and reduction of lipolysis in adipose tissue.[2] Some adenosine derivatives, such as A_1 AR agonists, are in clinical trials for treatment of cardiac arrhythmias and neuropathic pain.[1] However, the cardiovascular side effects and other side effects induced by the A_1 activation limit the clinical applications of A_1 agonists.

To address the problem of side effects, several purine ribofuranoside derivatives have been investigated as A_1 partial agonists endowed with a potentially more favorable clinical suitability.[3] In order to identify highly selective agonists at A_1 AR vs the other receptor subtypes, a wide range of adenosine derivatives modified at the C2,N^6-positions of the nucleobase and/or at the ribose moiety have been reported. Between the di- or trisubstituted adenosine derivatives, some N^6-cycloalkyl or bicycloalkyl derivatives and 5′-chloro-5′-deoxy analogues were found to have high affinity and selectivity for rat A_1 AR,[4] while some N^6-substituted-5′-alkylthio- or 5′-arylthio-analogues proved to be partial agonists for this AR subtype.[5] Among these, N^6-tetrahydrofuranyl-5′-(2-fluorophenylthio)-5′-deoxyadenosine showed affinity and partial agonism at the A_1 receptor in DDT cell membranes (hamster vas deferens smooth muscle cell line).[5b] Therefore, the 5′-hydroxyl group in adenosine analogues does not appear to be essential for receptor binding and activation of A_1 AR; furthermore, 5′-modified selective A_1 agonists could be more druggable than 5′-unmodified analogues, since normal ribonucleosides may be phosphorylated by adenosine kinases and in consecutive steps by nucleotide kinases to 5′-mono-, 5′-di-, or 5′-triphosphate derivatives, respectively, and subsequently interact with P2Y receptors and/or other biological targets. Moreover, the replacement of the 5′-hydroxyl group by a chlorine atom confers to these nucleosides greater stability versus purine nucleoside metabolizing enzymes such as adenosine deaminase and purine nucleoside phosphorylase.[6]

Based on these findings, in the search for new potent and selective human A_1 AR agonists, we synthesized a series of 5′-chloro- and 5′-(2-fluorophenylthio)-5′-deoxy derivatives of the selective A_1 AR agonists CPA,[a] CCPA, 2′-Me-CPA, 2′-Me-CCPA, and N^6-(±)-*endo*-norborn-2-yl purine ribonucleoside analogues that were evaluated for affinity and selectivity at all cloned human adenosine receptor subtypes (Chart 1).

Results and Discussion

Chemistry. The synthesis of compound **4** is outlined in Scheme 1. Treatment of 2,6-dichloro-9*H*-(2,3,5-tri-*O*-acetyl-β-

* To whom correspondence should be addressed. Phone: +39-0737-402233. Fax +39-0737-637345. E-mail: mario.grifantini@unicam.it.
[†] University of Camerino.
[‡] University of Naples "Federico II".
[§] Universität Würzburg.
[∥] Second University of Naples.

[a] Abbreviations: CPA, N^6-cyclopentyladenosine; CCPA, 2-chloro-N^6-cyclopentyladenosine; 2′-Me-CPA, 2′-*C*-methyl-N^6-cyclopentyladenosine; 2′-Me-CCPA, 2-chloro-2′-*C*-methyl-N^6-cyclopentyladenosine; (±)-ENBA, N^6-(±-*endo*-norborn-2-yl)adenosine; 5′-Cl-CPA, 5′-chloro-5′-deoxy-N^6-cyclopentyladenosine; 5′-Cl-CCPA, 2,5′-dichloro-5′-deoxy-N^6-cyclopentyladenosine; NECA, 5′-*N*-ethylcarboxamidoadenosine; HEMADO, 2-(hexyn-1-yl)-N^6-methyladenosine; 5′Cl5′d-(±)-ENBA, 5′-chloro-5′-deoxy-N^6-(±-*endo*-norborn-2-yl)adenosine; DPCPX, 8-cyclopentyl-1,3-dipropylxanthine; CHO, Chinese hamster ovary; TM, transmembrane helical domain; β_2-AR, β_2-adrenergic receptor.

10.1021/jm801456g CCC: $40.75
Published on Web 03/24/2009

Chart 1. Chemical Structures of Compounds **1**−**14**

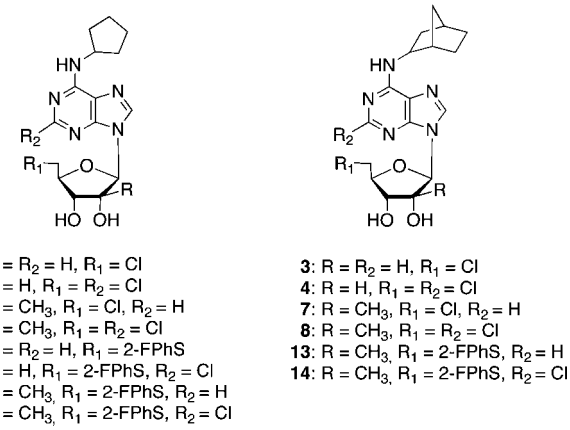

Scheme 1[a]

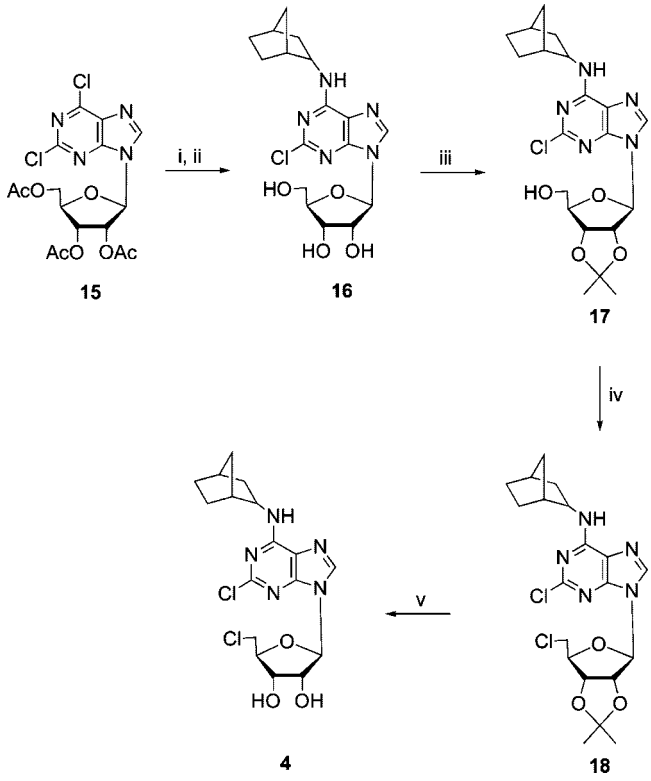

[a] Reagents and conditions: (i) (±)-*endo*-2-norbornylamine hydrochloride, TEA, EtOH, Δ; (ii) NH_3/MeOH, room temperature; (iii) 2,2-dimethoxypropane, camphorsulfonic acid, $(CH_3)_2CO$, Δ; (iv) $SOCl_2$, pyridine, CH_3CN, −5 °C to room temperature; (v) HCOOH (70%), 40 °C.

D-ribofuranosyl)purine (**15**), prepared as reported by Hou et al.,[7] with (±)-*endo*-norborn-2-yl-amine hydrochloride in the presence of triethylamine in absolute ethanol, followed by sugar deblocking with methanolic ammonia, gave 2-Cl-(±)-ENBA (**16**). Compound **16** was protected as 2′,3′-isopropylidene derivative **17** using camphorsulfonic acid and 2,2-dimethoxypropane in acetone in 80% yield. Conversion of **17** to 5′-chloro derivative **18** was performed by treatment with a mixture of thionyl chloride, pyridine, and acetonitrile. Finally, deprotection of **18** with 70% formic acid at 40 °C furnished compound **4**. Direct conversion of 2-Cl-(±)-ENBA (**16**) into its 5′-chloro-5′-deoxy derivative **4** using thionyl chloride and pyridine in acetonitrile or thionyl chloride and hexamethylphosphoramide (HMPA) was also tried, but low yields of **4** were obtained.

The synthesis of compounds **5**−**8** begins with the 6-chloro- or 2,6-dichloro-9*H*-(2-*C*-methyl-2,3,5-tri-*O*-benzoyl-β-D-ribofuranosyl)purine (**19** and **20**, respectively),[8] which was reacted with cyclopentylamine or (±)-*endo*-norborn-2-ylamine followed by sugar deblocking in basic conditions (Scheme 2). Compounds **21**−**24** were converted to the corresponding 2′,3′-isopropylidene derivatives **25**−**28**. 5′-Chlorination of **25**−**28**, followed by deisopropylidenation of **29**−**32**, gave the desired compounds **5**−**8**. 5′-(2-Fluorophenylthio) derivatives **11**−**14** were prepared by reaction of **29**−**32** with 2-fluorothiophenol in anhydrous DMF in the presence of 60% sodium hydride, with removal of the isopropylidene protecting group. 2-Chloro-N^6-cyclopentyl-5′-(2-fluorophenylthio)-5′-deoxyadenosine (**10**) was synthesized in a similar way starting from the 2′,3′-*O*-isopropylidene derivative of CCPA (**38**), which was prepared from CCPA[9] (**37**) (Scheme 3). Compounds 5′-Cl-CCPA (**2**), (±)-ENBA, and 5′Cl5′d-(±)-ENBA (**3**) were synthesized as reported in the literature.[4a,10] 5′-Cl-CPA (**1**), previously reported by van der Wenden et al.,[5a] N^6-cyclopentyl-5′-(2-fluorophenylthio)-5′-deoxyadenosine (**9**), and N^6-tetrahydrofuranyl-5′-(2-fluorophenylthio)-5′-deoxyadenosine (**41**), reported by Morrison et al.,[5b] were also prepared following a different route, in order to evaluate their affinity at human ARs (see the Supporting Information).

Binding Studies. The new compounds were evaluated at the human recombinant adenosine receptors, stably transfected into Chinese hamster ovary (CHO) cells, utilizing radioligand binding assays (A_1, A_{2A}, and A_3) or the adenylyl cyclase activity assay (A_{2B}).[3a,11,12] [^{3}H]CCPA, [^{3}H]NECA, and [^{3}H]HEMADO were used as radioligands for human A_1, A_{2A}, and A_3 ARs, respectively. In the case of the A_{2B} receptor subtype, K_i values were calculated from IC_{50} values determined by inhibition of NECA-stimulated adenylyl cyclase activity.[11]

Adenosine derivatives **1**−**3**, **9**, and **41** were assayed at the human recombinant adenosine receptors, since their affinities at human ARs have not been reported so far. The affinity and selectivity of the compounds were compared to those of the reference compounds CPA, CCPA, 2′-Me-CPA, 2′-Me-CCPA, and (±)-ENBA (Table 1).

Among the tested compounds, only **1**, **2**, **3**, and (±)-ENBA showed interaction with the hA_{2B} receptor with K_i values of 3.2, 4.8, 2.7, and 4.9 μM, respectively.

Compounds **1**−**8**, **23**, and **24** showed high affinity and selectivity for the human A_1 receptor. The 5′-chloro-5′-deoxy derivatives of CPA (5′-Cl-CPA, **1**) and (±)-ENBA (5′Cl5′d-(±)-ENBA, **3**) displayed the highest affinity at subnanomolar range for the hA_1 AR (K_i = 0.5 nM) and relevant selectivity vs hA_{2A} and hA_3 ARs. Among all tested compounds, 5′Cl5′d-(±)-ENBA (**3**) showed the highest selectivity for hA_1 vs hA_3 AR (2530-fold). At the same receptor subtype, the corresponding 2-chloro analogues (compounds **2** and **4**) showed a slightly lower affinity and selectivity. A similar modification in the ribose-modified *C*2′-methyl analogues resulted in a moderate decrease in affinity at all human AR subtypes; however, these compounds showed an A_1 selectivity similar to that of parent adenosine analogues.

These data are in accord with that previously reported by us for the *C*2′-methyl analogues of N^6-substituted adenosine that were found to have a decreased affinity, in particular at A_3 ARs, resulting in more A_1 selective agonists[4b,8] (e.g., compare CPA and (±)-ENBA with 2′-Me-CPA and **23**, respectively). Among the 5′-chloro-5′-deoxy- and 2,5′-dichloro-5′-deoxy-*C*2′-methyladenosine derivatives, the most interesting compounds appeared to be the N^6-(±)-*endo*-norbornyl analogues **7** and **8**, which

Scheme 2[a]

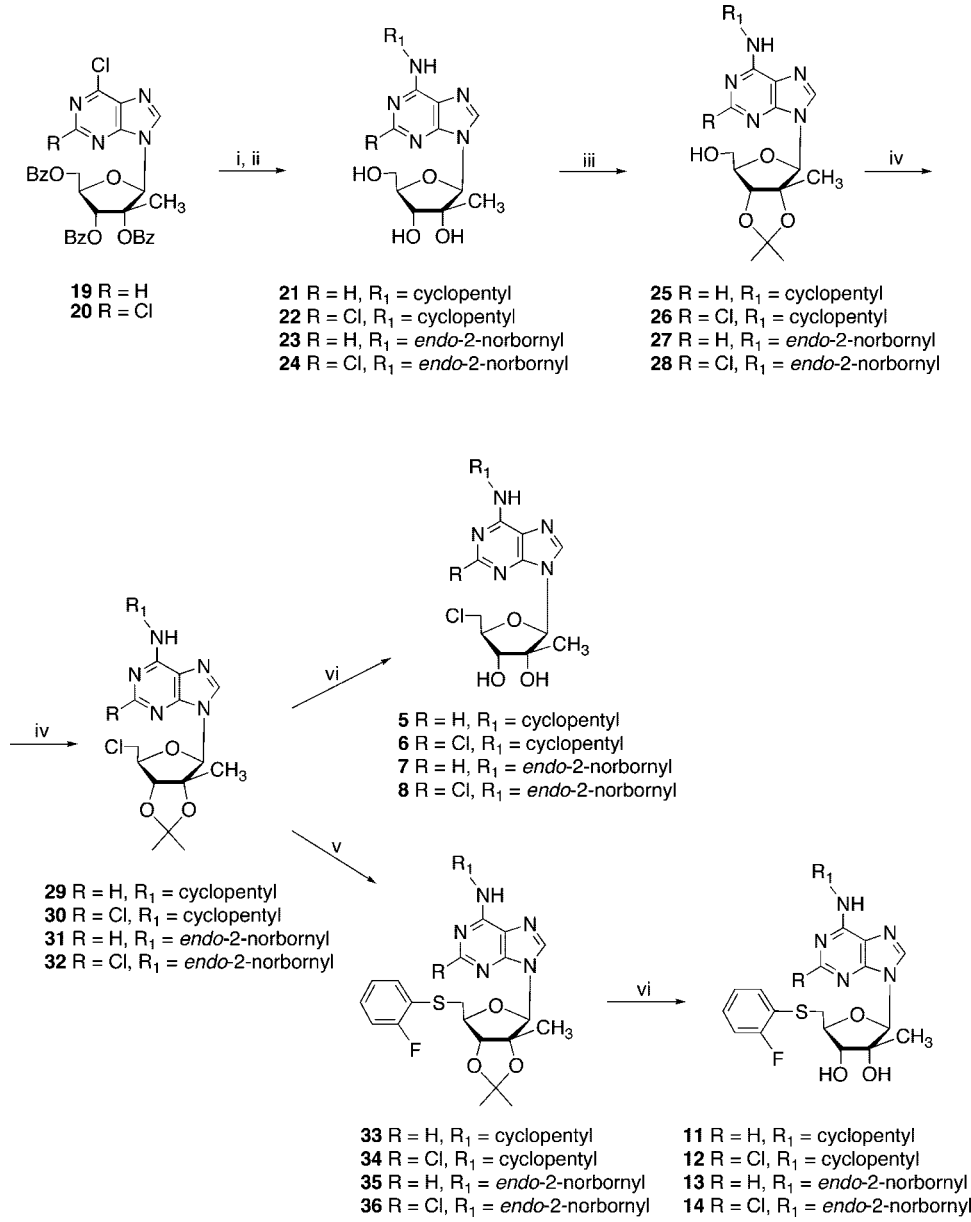

[a] Reagents and conditions: (i) R_1NH_2, EtOH, Δ; (ii) NH_3/MeOH, room temperature; (iii) 2,2-dimethoxypropane, camphorsulfonic acid, $(CH_3)_2CO$, Δ; (iv) $SOCl_2$, pyridine, CH_3CN, −5 °C to room temperature; (v) NaH 60%, 2-fluorothiophenol, DMF, 0 °C to room temperature; (vi) HCOOH (70%), 40 °C.

showed good A_1 affinity (K_i = 9.13 and 9.16 nM, respectively) and A_1 selectivity, vs A_{2A} = 2630 and 3450, and vs A_3 = 1270 and 644, respectively.

As far as it concerns the 5′-(2-fluorophenylthio) substitution, the N^6-cyclopentyl derivative **9** was the most affine compound at the hA_1 receptor with a K_i of 64.7 nM and with A_{2A}/A_1 and A_3/A_1 selectivities lower than those of the parent compounds CPA and 5′-Cl-CPA (**1**), while the N^6-tetrahydrofuranyl analogue **41** displayed 3.9-fold lower affinity and a similar selectivity. The introduction of a chlorine in the 2-position of the purine ring (compound **10**) induced a slight decrease of the affinity at the hA_1 and hA_3 receptors and slightly enhanced the affinity at the hA_{2A} receptor. The 2′-*C*-methyl modification in these compounds and in the N^6-(±)-*endo*-2-norbornyl analogues (compounds **11**−**14**) brought about a reduction of affinity at all receptor subtypes.

Adenylyl Cyclase Activity. The ability of selected compounds (**1**, **2**, **3**, **4**, **23**, (±)-ENBA, and 2-Cl-(±)-ENBA) to inhibit forskolin-stimulated cAMP production via the human A_1 receptor was studied in comparison with the full agonist CCPA. The functional assay showed that all these compounds are full agonists on the basis of their adenylyl cyclase inhibitory activity, which was comparable to that of CCPA (Figure 1). The ability of the selected compounds **1**, **3**, CPA, and (±)-ENBA to inhibit forskolin-stimulated cAMP production via human A_3 AR was studied in comparison with the A_3 agonist NECA. The functional assay showed that the 5′-chloro-5′-deoxy derivatives **1** and **3** behave as antagonists, while the corresponding parent compounds CPA and (±)-ENBA are partial agonists compared with NECA, which proved to be a full agonist (Figure 2).

Molecular Modeling. In order to explain why the replacement of the OH group in the 5′-position in N^6-substituted adenosine analogues with a chlorine is tolerated at hA_1 AR but is scarcely tolerated at hA_3 AR, a molecular docking analysis of CPA, (±)-ENBA, and compounds **1** and **3** was performed at the homology models of both ARs built using the bovine rhodopsin (b-Rho) crystal structure as a template.[13] In the last

Scheme 3[a]

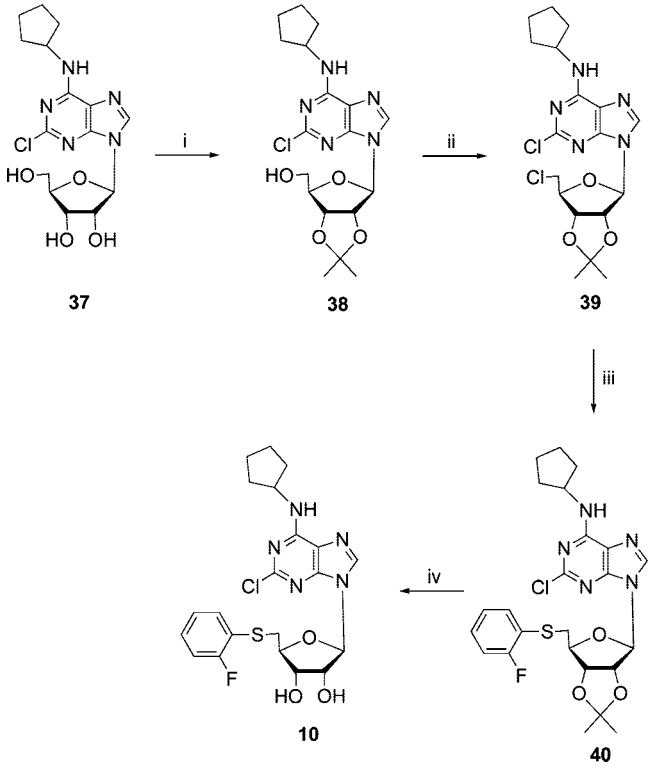

[a] Reagents and conditions: (i) 2,2-dimethoxypropane, camphorsulfonic acid, $(CH_3)_2CO$, Δ; (ii) $SOCl_2$, pyridine, CH_3CN, −5 °C to room temperature; (iii) NaH 60%, 2-fluorothiophenol, DMF, 0 °C to room temperature; (iv) HCOOH (70%), 40 °C.

14 years, many AR models were published, reporting also the docking of agonists and antagonists.[14] Indeed, the use of the b-Rho X-ray structure[13] has led to a great improvement in the results. Unfortunately, this structure that serves as template for GPCR models was obtained for its ground-state only. For this reason, there is an opinion that rhodopsin-based homology modeling of GPCRs is more applicable for studying antagonist than agonist binding modes. Until now, there is only a rough picture of the conformational changes that occur during receptor activation. Ballesteros et al.[14f] suggested that receptor activation could be due to a different rearrangement of TM3 and TM6. Furthermore, on the basis of UV absorption analysis, it has been suggested that when b-Rho is activated, the χ_1 rotamer of the high conserved residue W265 (6.48) shifts from *gauche*$^+$ to *trans*.[15] Thus, the intramolecular contact network might be destabilized, inducing a characteristic anticlockwise movement of TMs III, VI, and VII from the extracellular view to activate the receptor. Recently, Kobilka et al.[16] reported the first X-ray structure of the human β_2-adrenergic receptor (β_2-AR). The data show that the overall topologies of b-Rho and β_2-AR are quite similar. The root-mean-square deviation (rmsd) for the Cα backbone of the transmembrane region between rhodopsin and β_2-AR is 1.56 Å, which indicates a very similar arrangement of the TM helices. This feature also supports the previous notion of a conserved activation mechanism, i.e. an agonist-induced conformational rearrangement, across this class of GPCRs. However, the β_2-AR shows a more open structure, especially in the lower ends of TM3 and TM6. The authors suggest that this feature could be the basis for the observed basal activity observed for many GPCRs. It is also noteworthy that the current structure of the β_2-AR is an inactive state and may, therefore, only be useful for identifying inverse agonists and antagonists.

Because of the difficulty to generate a fully active conformation (e.g., Meta II of b-Rho) for analyzing agonist binding, the binding preference of agonists CPA, (±)-ENBA, **1**, and **3** to the Meta I conformation of both hA_1 AR and hA_3 AR was studied. The agonist-bound conformation, in a form resembling the not fully activated Meta I state of b-Rho, was obtained by modeling the rearrangement of the side chain of W265 (6.48), as described in the Experimental Section. Although the Meta I state is still far more similar to the resting conformation than to the presumed yet undisclosed fully active conformation, this state structure is preferable to the ground-state structure for agonist docking.

To assess the dynamic stability of the obtained complexes and to analyze the potential ligand−receptor interactions, a molecular dynamics (MD) simulation of 1 ns at a constant temperature of 300 K was run. The distances between the ligands and the key receptor residues were monitored along the complete MD trajectory. The results of docking and MD simulations performed for compounds CPA, (±)-ENBA, **1**, and **3** indicated that the adenine moiety of the ligands had a similar position and orientation inside the putative hA_1 AR binding site, defined by TMIII, TMV, TMVI, and TMVII. In particular, the N^6-substituent of the ligands was oriented toward TMV, whereas the ribose ring was placed between helices TMIII and TMVII with the 5′-substituent pointing toward the intracellular part of the receptor. Figures 3 and 4 show the binding mode of CPA, (±)-ENBA, **1**, and **3** into the hA_1 AR model as the average structure calculated on the last 200 ps of the production step.

All four ligands adopted a stable binding pose during the simulation time, forming almost the same interactions with hA_1 AR. Interestingly, these interactions were very stable throughout the MD simulation, thus explaining the high potency of CPA (K_i = 2.25 nM), (±)-ENBA (K_i = 0.54 nM), **1** (K_i = 0.59 nM), and **3** (K_i = 0.51 nM) toward hA_1 AR. In agreement with the published data of molecular modeling and site-directed mutagenesis of the AR family,[14d,17−19] the 3′-OH and 2′-OH groups were H-bonded to T277 (7.42) and H278 (7.43), respectively. The histidine residue is conserved among all ARs, and support for it being a critical recognition element has come from diverse approaches.[14e,20−22] For example, H278 (7.43) is important for agonist but not antagonist binding for the A_1, A_{2A}, and A_3 ARs. The N^6-amino group was found to establish H-bonds with the CO oxygen of N254 (6.55) side chain. The N^1 nitrogen of **1** also formed a H-bond with the N254 (6.55) NH group. This residue, conserved among all adenosine receptor subtypes, was found to be important for ligand binding. In fact, the inability of the N250A mutant hA_3 AR[23] or the corresponding mutant A_{2A} AR[20] to bind either radiolabeled agonist or antagonist was consistent with a proposed direct interaction of this residue with our ligands. Moreover, both cyclopentyl and norbornyl N^6-substituents were favorably located in a pocket formed by several hydrophobic residues including L88 (3.33), M180 (5.38), V181 (5.39), F185 (5.43), and L258 (6.59). In addition, it was found that the 5′-OH of CPA and (±)-ENBA accepted a H-bond from the T91 (3.36) OH group, in line with the site mutagenesis studies, which indicate that mutation of this residue to alanine in the A_1 and A_{2A} receptors, respectively, substantially decreases agonist affinity.[24,25]

The chlorine atom at the 5′-position in compounds **1** and **3** was too far away from the T91 (3.36) OH group to form an effective H-bond. Nevertheless, MD simulations indicated that it could still accept a H-bond from the W247 (6.48) indole NH, thus explaining the high hA_1 AR affinity displayed by these compounds. The importance of W265 (6.48) in b-Rho activation

Table 1. Binding Affinity at Human A_1, A_{2A}, A_{2B}, and A_3 Adenosine Receptor Subtypes

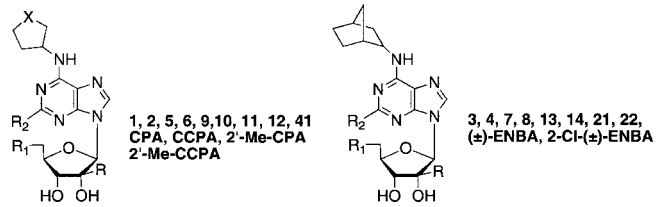

					K_i (nM)				selectivity	
compd	R	R_1	R_2	X	A_1[a]	A_{2A}[b]	A_{2B}[c]	A_3[b]	A_{2A}/A_1	A_3/A_1
1	H	Cl	H	CH_2	0.59	837	3,210	376	1,470	637
2	H	Cl	Cl	CH_2	1.56	2,160	4,830	417	1,380	267
3	H	Cl	H		0.51	1,340	2,740	1,290	2,630	2,530
4	H	Cl	Cl		1.61	2,050	>10,000	1,410	1,270	875
5	CH_3	Cl	H	CH_2	28.4	>100,000	>10,000	6,740	>3,520	237
6	CH_3	Cl	Cl	CH_2	12.8	16,200	>10,000	3,030	1,770	237
7	CH_3	Cl	H		9.13	24,000	>10,000	11,600	2,630	1,270
8	CH_3	Cl	Cl		9.16	31,600	>10,000	5,900	3,450	644
9	H	2FPhS	H	CH_2	64.7	5,170	>10,000	296	80	5
10	H	2FPhS	Cl	CH_2	258	2,190	>10,000	479	8	2
11	CH_3	2FPhS	H	CH_2	1,680	>100,000	>10,000	1,440	>60	0.9
12	CH_3	2FPhS	Cl	CH_2	2,150	>100,000	>10,000	1,150	>47	0.5
13	CH_3	2FPhS	H		1,060	>100,000	>10,000	3,480	>94	3
14	CH_3	2FPhS	Cl		2,970	>100,000	>10,000	4,350	>34	1.5
41	H	2FPhS	H	O	250	18,900	>10,000	746	76	3
23	CH_3	OH	H		4.09	8,780	>10,000	2,520	2,150	616
24	CH_3	OH	Cl		6.96	11,800	>10,000	4,490	1,700	645
CPA[d]	H	OH	H	CH_2	2.25	794	18,600	43	353	19
CCPA[d]	H	OH	Cl	CH_2	0.8	2,300	18,800	42	2,875	53
(±)-ENBA	H	OH	H		0.54	1,270	4,930	101	2,350	187
16 2-Cl-(±)-ENBA	H	OH	Cl		0.71	797	>10,000	129	1,120	182
2′-Me-CPA[d]	CH_3	OH	H	CH_2	4.5	10,400	26,800	879	2,301	195
2′-Me-CCPA[d]	CH_3	OH	Cl	CH_2	3.3	9,580	37,600	1,150	2,903	348

[a] Displacement of [^{3}H]CCPA binding in CHO cells stably transfected with the human recombinant A_1 adenosine receptor. [b] Displacement of [^{3}H]NECA binding in CHO cells stably transfected with human recombinant A_1 or A_3 adenosine receptors. [c] K_i values were calculated from IC_{50} values determined by inhibition of NECA-stimulated adenylyl cyclase activity. [d] Data are from ref 3a.

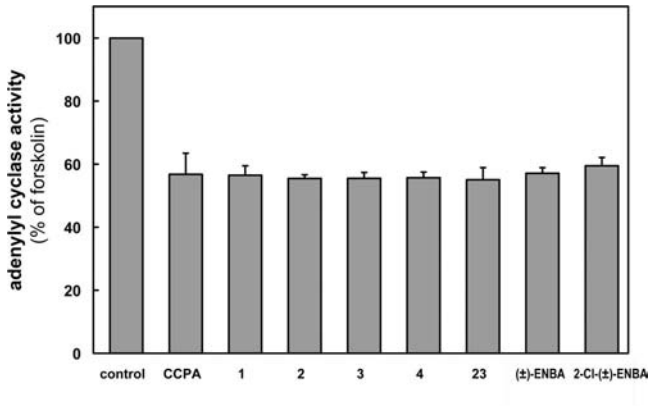

Figure 1. Inhibition of adenylyl cyclase activity via the human A_1 adenosine receptor by selected compounds. The percentage of activity remaining after agonist-mediated inhibition of 10 μM forskolin-stimulated cyclase activity (100%) is shown. Data are means (±SEM) of three independent experiments.

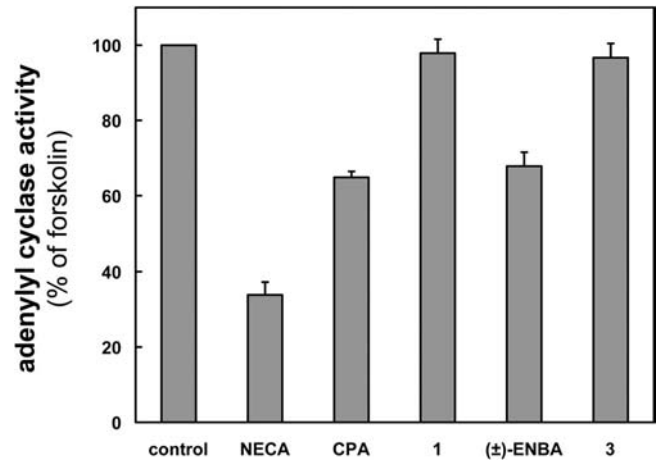

Figure 2. Inhibition of adenylyl cyclase activity via the human A_3 adenosine receptor by selected compounds. The percentage of activity remaining after agonist-mediated inhibition of 10 μM forskolin-stimulated cyclase activity (100%) is shown. Data are means (±SEM) of three independent experiments.

was suggested in a UV−visible spectroscopic analysis of site-directed mutagenesis of this residue. The differential absorbance indicated that perturbations in the characteristics of W126 (3.41) and W265 (6.48) resulted from a general conformational change concomitant with Meta II formation.[15] There was a rearrangement close to the bend of TM6 upon Meta I formation. The electron density featured a significant deviation from the position of W265 (6.48) in the ground-state structure, suggesting the possibility of movement of W265 (6.48). Meta I formation involved no large rigid-body movements or rotations of helices from their position in the ground-state. Instead, changes seemed to be localized, probably involving movement of side chains such as W265 (6.48) in kinked regions of helices close to the retinal-binding pocket.[26] Before the MD simulation of the ligand/hA_1 AR complexes, W247 (6.48) was in the *gauche*$^-$ χ_1 configuration, as described in the Experimental Section. During the MD simulation, the rotamer of W247 (6.48) spontaneously shifted from *gauche*$^-$ χ_1 to *trans* χ_1 ($\chi_1 = -164$ for CPA, $\chi_1 = -168$ for (±)-ENBA, $\chi_1 = -168$ for **1**, and $\chi_1 = -155$ for **3**),

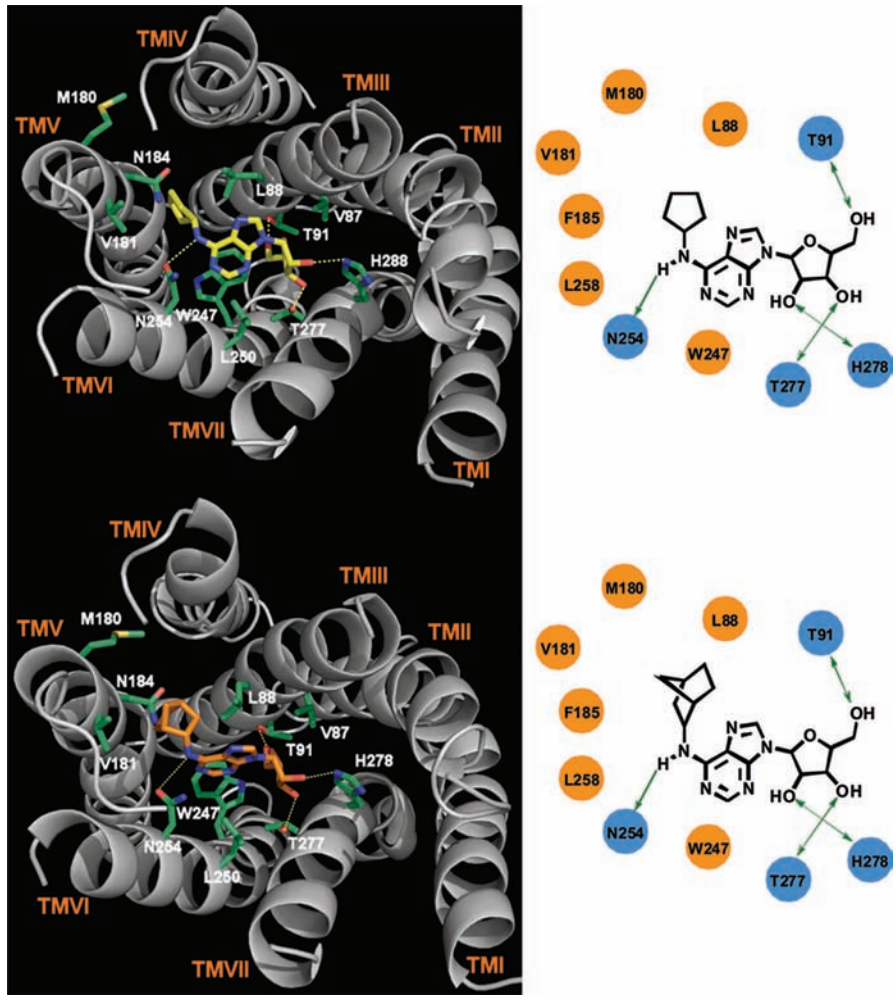

Figure 3. On the left, (extracellular) view of CPA (top, yellow) and (±)-ENBA (bottom, orange) complexed with the hA_1 AR model. For clarity, only interacting residues are displayed. Ligands and interacting key residues (green) are represented as stick models, while the protein is represented as gray ribbons. H-bonds are shown as dashed yellow lines. On the right, schematic representation of the binding mode of CPA (top) and (±)-ENBA (bottom) obtained after docking and MD simulations. The green arrows correspond to the putative H-bonds. The critical residues involved in interactions with the ligand are colored in blue.

that is generally assumed to be stabilized by agonist binding and indicative of an activated receptor.[26,27]

Examination of the optimized models of the CPA/hA_3 AR and (±)-ENBA/hA_3 AR complexes (Figure 5) showed that the purine ring of the ligands was surrounded by a hydrophobic pocket defined by L91 (3.33) and L246 (6.51). The N^6-cyclopentyl and norbornyl substituents appeared to be wedged between TMV and TMVI, interacting with hydrophobic residues F182 (5.43), I186 (5.47), M172 (5.32), M177 (5.38), and V178 (5.39). In addition, the N^6-nitrogen was located within H-bonding distance from the C═O oxygen of N250 (6.55). The 5′-OH group also donated a H-bond to the T94 (3.36) OH oxygen. Only the 2′-OH substituent of CPA established a further H-bond with S271 (7.42), while the 2′-OH of (±)-ENBA did not seem to interact with S271 (7.42). Moreover, the 3′-OH substituent of both ligands was away from the H272 (7.43) imidazole ring to make an efficient H-bond. In fact, from the MD trajectories (data not shown), it can be deduced that these H-bonds, initially present in the complex, were gradually lost during the whole length of the monitored simulation. These results are consistent with 10-fold and 1000-fold lower affinity of CPA and (±)-ENBA, respectively, toward hA_3 AR, in comparison with the corresponding binding affinity of these compounds toward hA_1 AR.

Different results were obtained when analyzing the trajectories of **1** and **3** in complex with the hA_3 AR. With the exception of the H-bond formed between the NH^6 group of the ligands and the CO oxygen of the N254 side chain, which remained quite stable during all the simulation period (the $N^6\cdots O{=}C$ distance was ~3.0 Å), the remaining polar interactions were not strong enough to be preserved throughout the MD simulation, giving average distances longer than that of an ideal H-bond. In particular, the **3**/hA_3 complex turned out to be highly unstable during the MD simulation. The ligand considerably changed its position at the hA_3 AR binding site and was oriented parallel to the transmembrane domain axis already after a few hundred picoseconds. This was probably due to the inability of the chlorine atoms of **1** and **3** to make a H-bond to T94 (3.36), unlike the cases of CPA and (±)-ENBA, which possess a 5′-OH group that, in contrast, is able to form this interaction. Thus, the incapability of the 5′-Cl atom of **1** and **3** to form a H-bond to T94 (3.36), which is a key receptor anchoring point for the hA_3 AR agonists,[28] together with the sterically bulky substituents at the N^6 position of the adenine ring might change the optimal binding mode of the ligand, thereby decreasing the relative stability of the complexes. This finding is in accordance with the drastic reduction of affinity of **1** and **3** toward hA_3 AR. Moreover, it is important to note that during the MD simulation

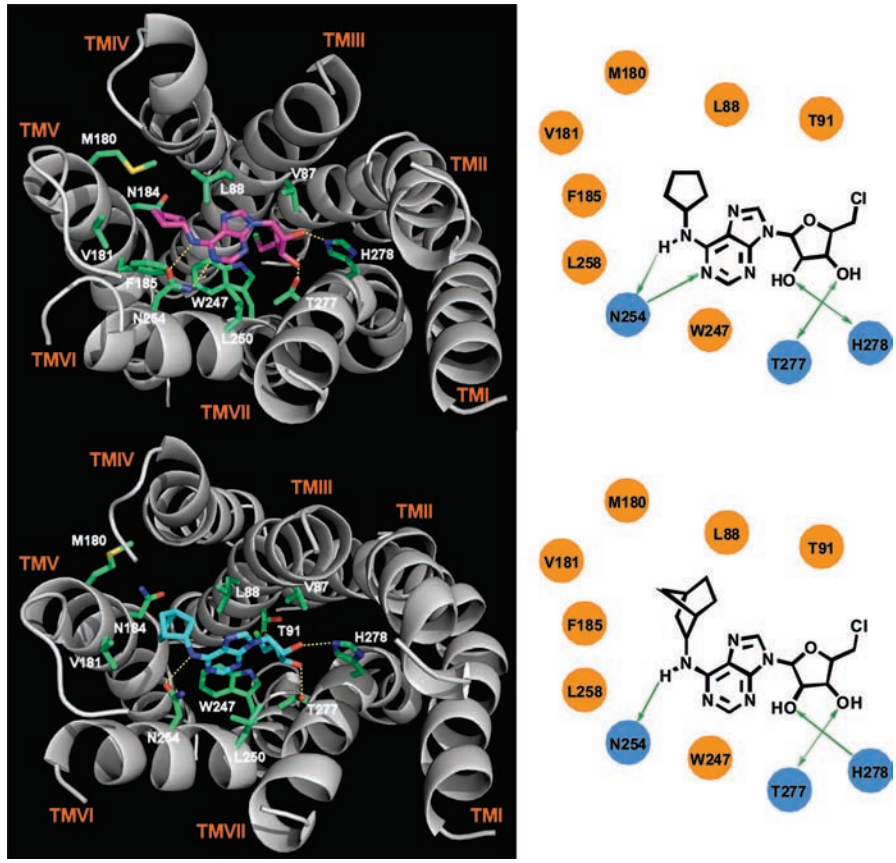

Figure 4. On the left, (extracellular) view of compounds **1** (top, magenta) and **3** (bottom, cyan) complexed with the hA_1 AR model. For clarity, only interacting residues are displayed. Ligands and interacting key residues (green) are represented as stick models, while the protein is represented as gray ribbons. H-bonds are shown as dashed yellow lines. On the right, schematic representation of the binding mode of **1** (top) and **3** (bottom) obtained after docking and MD simulations. The green arrows correspond to the putative H-bonds. The critical residues involved in interactions with the ligand are colored in blue.

of both **1**/hA_3 and **3**/hA_3 complexes, in sharp contrast to **1**/hA_1 and **3**/hA_1 complexes, the χ_1 rotamer of residue W243 (6.48) unexpectedly shifted from the *gauche*$^-$ to the *gauche*$^+$ conformation ($\chi_1 = -69$ for **1** and $\chi_1 = -80$ for **3**), indicative of an "inactive" state of the receptor. This result nicely explains the observed low intrinsic efficacy of **1** and **3** at hA_3 AR in comparison with the high efficacy of the same ligands at hA_1 AR.

Antinociceptive Effect. To investigate the therapeutic potential of 5′Cl5′d-(±)-ENBA (**3**), we have evaluated its analgesic activity in mice in comparison with (±)-ENBA using the formalin test. Formalin injection induces a biphasic stereotypical nocifensive behavior.[29] Nociceptive responses are divided into an early, short lasting first phase (0−7 min) caused by a primary afferent discharge produced by the stimulus, followed by a quiescent period and then a second, prolonged phase (15−60 min) of tonic pain. Systemic administration of 5′Cl5′d-(±)-ENBA (1−2 mg/Kg, i.p.), 10 min before formalin, reduced the late nociceptive behavior induced by formalin in a dose-dependent manner ($P < 0.005$). The highest dose of 5′Cl5′d-(±)-ENBA used (2 mg/Kg) reduced both the early and the late phases of the formalin test, and this effect was prevented by DPCPX (3 mg/kg, i.p.), a selective A_1 receptor antagonist (Figure 6). The antinociceptive effect of 5′Cl5′d-(±)-ENBA proved to be comparable to that of 2′-Me-CCPA.[30] Systemic administration of (±)-ENBA (0.3−1 mg/kg, i.p.), 10 min before formalin injection, completely erased both the early and the late phases of the formalin-induced nociceptive behavior ($P < 0.005$) (Figure 7). The lower antinociceptive effect displayed by 5′Cl5′d-(±)-ENBA compared to that of (±)-ENBA is quite surprising because these compounds displayed similar affinity and efficacy profiles at both human and rat[4a] A_1 AR. Furthermore, 5′Cl5′d-(±)-ENBA could have more favorable blood−brain transport characteristics owing to its higher lipophilicity (**3**: log*P* = 1.04 vs (±)-ENBA: log *P* = −0.14). Further research is needed to verify if the higher activity of (±)-ENBA is due to its metabolic conversion to nucleotide derivatives that could trigger different signaling pathways or to the lower metabolic stability of 5′Cl5′d-(±)-ENBA.

Conclusions

In summary, we synthesized a series of 5′-chloro-5′-deoxy-N^6-cycloalkyl(bicycloalkyl)adenosine and 2′-*C*-methyladenosine derivatives to evaluate their affinity and efficacy at human A_1, A_{2A}, A_{2B}, and A_3 adenosine receptor subtypes. Biological data confirmed that the replacement of the 5′-hydroxyl group by a chlorine atom in the β-D-ribofuranose ring in N^6-substituted adenosine derivatives is well tolerated by the human A_1 receptor but less tolerated by other human receptor subtypes; therefore, this modification represents an effective strategy to increase the selectivity for hA_1 AR.

In the series of N^6-cyclopentyl- and (*endo*-norborn-2-yl)adenosine derivatives, 5′-chloro-5′-deoxy-CPA (**1**) and 5′-chloro-5′-deoxy-(±)-ENBA (**3**) displayed the highest hA_1 affinity in the subnanomolar range and significant hA_1 selectivity. The corresponding derivatives of 2′-*C*-methyladenosine showed a slight decrease of the affinity at all receptor subtypes but a similar or increased A_1 selectivity as compared to the adenosine

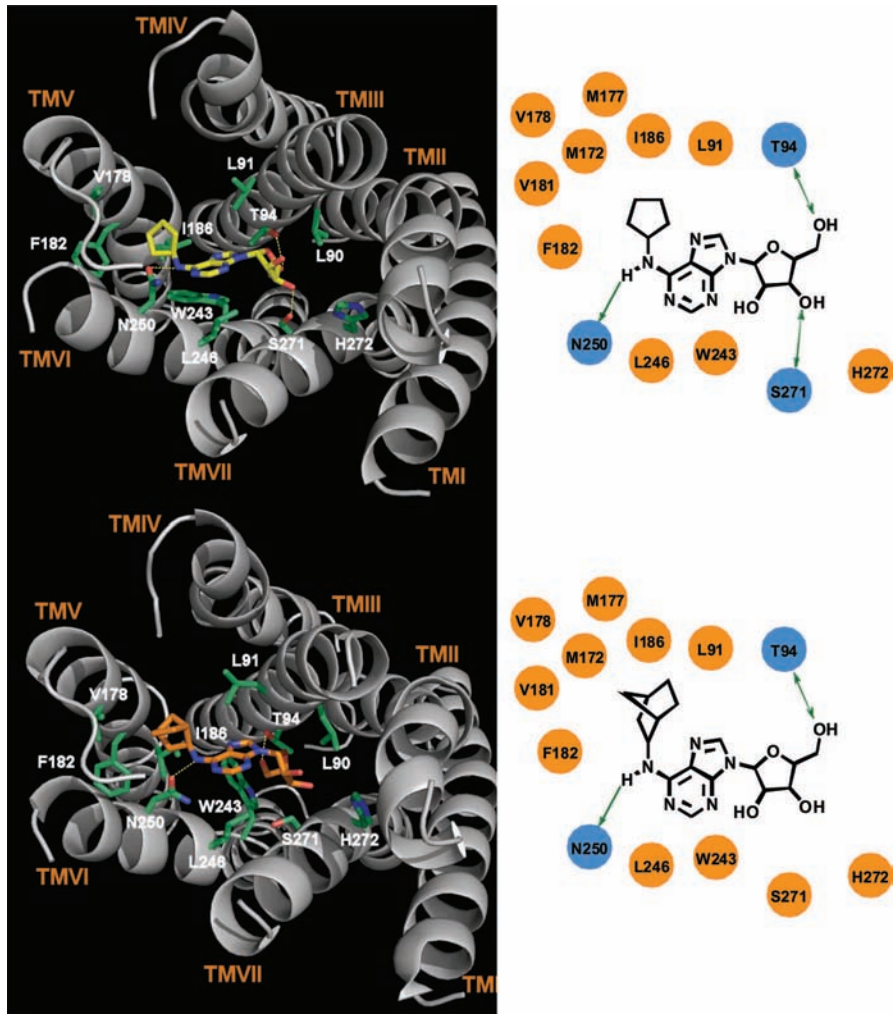

Figure 5. On the left, (extracellular) view of CPA (top, yellow) and (±)-ENBA (bottom, orange) complexed with the hA_3 AR model. For clarity, only interacting residues are displayed. Ligands and interacting key residues (green) are represented as stick models, while the protein is represented as gray ribbons. H-bonds are shown as dashed yellow lines. On the right, schematic representation of the binding mode of CPA (top) and (±)-ENBA (bottom) obtained after docking and MD simulations. The green arrows correspond to the putative H-bonds. The critical residues involved in interactions with the ligand are colored in blue.

analogues. The higher selectivity of 5′-chloro-5′-deoxy-modified adenosine derivatives for hA_1 AR vs hA_3 AR compared to that of the 5′-hydroxy parent compounds was rationalized by a molecular modeling study. In particular, it was pointed out that the 5′-Cl atom of compounds **1** and **3** is unable to form a H-bond to a T94 (3.36) residue, which is a key receptor anchoring point for the hA_3 AR agonists.

5′-Chloro-5′-deoxy-(±)-ENBA (**3**) was found to be effective in reverting formaline-induced nocifensive behavior in mice, albeit at a higher concentration than (±)-ENBA, confirming that pharmacological modulation of the hA_1 AR may play a critical role in pain modulation. Owing to the higher selectivity of 5′-chloro-5′-deoxy adenosine derivatives for the human A_1 receptor, this type of A_1 agonists deserves further investigation to explore their therapeutic potential.

Experimental Section

Chemistry. Thin layer chromatography (TLC) was run on silica gel 60 F_{254} plates (Merck); silica gel 60 (70−230 and 230−400 mesh, Merck) for column chromatography was used. ^{1}H NMR spectra were recorded on a Varian Mercury AS400 instrument. The chemical shift values are expressed in δ values (ppm), and coupling constants (*J*) are in hertz; TMS was used as an internal standard. The presence of all exchangeable protons was confirmed by addition of D_2O. Mass spectra were recorded on an HP 1100 series instrument. All measurements were performed in the positive ion mode using atmospheric pressure electrospray ionization (API-ESI). Partition coefficients (log *P*) were computed using the log *P* function implemented in ChemDraw Ultra version 10.0. Elemental analyses were determined on an EA 1108 CHNS-O (Fisons Instruments) analyzer and are within ±0.4% of theoretical values. CPA was purchased from Tocris Bioscience.

General Procedure for N^6-Amination (Compounds 16, 23, and 24). To a stirred solution of 2,6-dichloro-9*H*-(2,3,5-*O*-acetyl-β-D-ribofuranosyl)purine (**15**)[7] or 6-chloro-9*H*-(2-*C*-methyl-2,3,5-*O*-benzoyl-β-D-ribofuranosyl)purine[8] (**19**) or 2,6-dichloro-9*H*-(2-*C*-methyl-2,3,5-*O*-benzoyl-β-D-ribofuranosyl)purine[8] (**20**) (1.0 mmol) in absolute ethanol (20 mL), were added (±)-*endo*-norborn-2-ylamine hydrochloride (2.0 mmol), and anhydrous triethylamine (5.8 mmol). The reaction mixture was refluxed for the time reported below and concentrated in vacuo. The residue was dissolved in methanol saturated with ammonia (25 mL) and stirred at room temperature overnight. Evaporation of the solvent to dryness gave a residue which was purified by column chromatography.

2-Chloro-N^6-(±)-*endo*-norbornyl-9*H*-(β-D-ribofuranosyl)adenine (16). The title compound was obtained from **15** (reaction time 3 h). Chromatography on a silica gel column ($CHCl_3$−MeOH, 96:4) gave **16** as a white solid (90% yield). ^{1}H NMR (DMSO-d_6) δ 1.20−1.29 (m, 3H, norbornyl), 1.37−1.46 (m, 3H, norbornyl), 1.50−1.65 (2m, 1H, norbornyl), 1.83−1.91 (m, 1H, norbornyl),

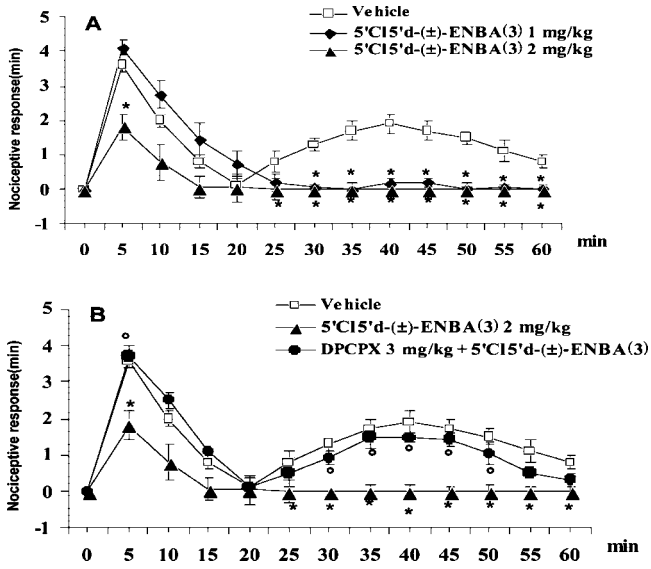

Figure 6. Effect of subcutaneous formalin (1.25%, 30 μL) injections into the hind paw of mice on the time course of the nociceptive behaviors. Formalin was injected 10 min after the systemic administration of vehicle (0.9% NaCl, i.p.) or drugs. Part A shows the effects of the systemic administration of 5′Cl5′d-(±)-ENBA (**3**) (1 and 2 mg/kg, i.p.). Part B shows the effects of the systemic administration of **3** (2 mg/kg, i.p.) in combination with DPCPX (3 mg/kg, i.p.). Recording of nociceptive behavior began immediately after the injection of formalin (time 0) and was continued for 60 min. Each point represents the total time of the nociceptive responses (mean ± S.E.M.) of 8 mice per group, measured every 5 min. * indicates significant differences versus vehicle, and ○ indicates significant differences versus 5′Cl5′d-(±)-ENBA. $P < 0.05$ was considered statistically significant.

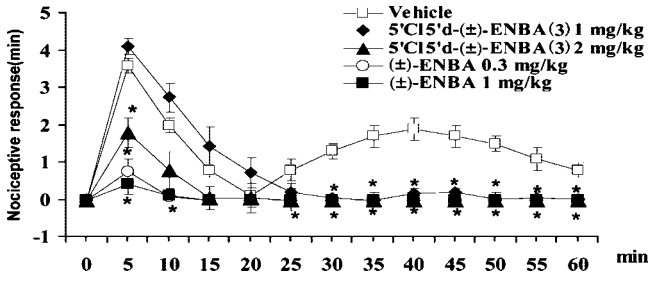

Figure 7. Effect of subcutaneous formalin (1.25%, 30 μL) injection into the hind paw of mice on the time course of the nociceptive behaviors. Formalin was injected 10 min after the systemic administration of vehicle (0.9% NaCl, i.p.), 5′Cl5′d-(±)-ENBA (**3**) (1 and 2 mg/kg, i.p.) or (±)-ENBA (0.3 and 1 mg/kg, i.p.). Recording of nociceptive behaviors began immediately after the injection of formalin (time 0) and was continued for 60 min. Each point represents the total time of the nociceptive responses (mean ± S.E.M.) of 8 mice per group, measured every 5 min. * indicates significant differences versus vehicle. $P < 0.05$ was considered statistically significant.

2.16 (br s, 1H, norbornyl), 2.52 (br s, 1H, norbornyl), 3.49−3.56 (m, 1H, H-5′), 3.61−3.67 (m, 1H, H-5′), 3.89−3.94 (m, 1H, H-4′), 4.10 (q, J = 4.9 Hz, 1H, H-3′), 4.20−4.27 (m, 1H, NHC*H*), 4.50 (q, J = 5.6 Hz, 1H, H-2′), 5.05 (t, J = 5.8 Hz, 1H, OH), 5.40 (d, J = 5.1 Hz, 1H, OH), 5.45 (dd, J = 3.2, 6.2 Hz, 1H, OH), 5.80 (d, J = 6.0 Hz, 1H, H-1′), 8.40 (s and d, 2H, NH, H-8). MS: *m*/*z* 396.7 $[M + H]^+$. Anal. ($C_{17}H_{22}ClN_5O_4$) C, H, N.

N^6-(±)-*endo*-Norbornyl-9*H*-(2-*C*-methyl-β-D-ribofuranosyl)-adenine (23). The title compound was synthesized from **19** (reaction time 3.5 h). Chromatography on a silica gel column ($CHCl_3$−MeOH, 93:7) gave **23** as a white solid (90% yield). ^{1}H NMR (DMSO-d_6) δ 0.78 (2s, 3H, CH_3), 1.20−1.36 (m, 3H, norbornyl), 1.38−1.48 (m, 3H, norbornyl), 1.56−1.66 (m, 1H, norbornyl), 1.84−1.94 (m, 1H, norbornyl), 2.16 (br s, 1H, norbornyl), 2.52 (s, 1H, norbornyl), 3.62−3.70 (m, 1H, H-5′), 3.78−3.84 (m, 1H, H-5′), 3.86−3.90 (m, 1H, H-4′), 4.02−4.10 (m, 1H, H-3′), 4.28−4.38 (m, 1H, NHC*H*), 5.15−5.25 (m, 3H, OH), 5.95 (s, 1H, H-1′), 7.75 (t, J = 6.0 Hz, 1H, NH), 8.18 (s, 1H, H-2), 8.45 (s, 1H, H-8). MS: *m*/*z* 376.5 $[M + H]^+$. Anal. ($C_{18}H_{25}N_5O_4$) C, H, N.

2-Chloro-N^6-(±)-*endo*-norbornyl-9*H*-(2-*C*-methyl-β-D-ribofuranosyl)adenine (24). The title compound was synthesized from **20** (reaction time 2 h) and purified by chromatography on a silica gel column ($CHCl_3$−MeOH, 97:3) as a white solid (97% yield). ^{1}H NMR (DMSO-d_6) δ 0.80 (2s, 3H, CH_3), 1.22−1.30 (m, 3H, norbornyl), 1.40−1.48 (m, 3H, norbornyl), 1.50−1.63 (2m, 1H, norbornyl), 1.82−1.88 (2m, 1H, norbornyl), 2.16 (br s, 1H, norbornyl), 2.52 (br s, 1H, norbornyl), 3.64−3.70 (m, 1H, H-5′), 3.78−3.84 (m, 1H, H-5′), 3.86−3.92 (m, 1H, H-4′), 4.0 (dd, J = 7.3, 9.0 Hz, 1H, H-3′), 4.20−4.28 (m, 1H, NHC*H*), 5.12−5.16 (m, 1H, OH), 5.22 (d, J = 6.4 Hz, 1H, OH), 5.32 (d, J = 3.4 Hz, 1H, OH), 5.82 (s, 1H, H-1′), 8.38 (t, J = 6.2 Hz, 1H, NH), 8.50 (s, 1H, H-8). MS: *m*/*z* 410.7 $[M + H]^+$. Anal. ($C_{18}H_{24}ClN_5O_4$) C, H, N.

General Procedure for the Synthesis of 2′,3′-*O*-Isopropylidene Derivatives 17, 27, 28, and 38. A mixture of **16**, **23**, **24**, or 2-chloro-N^6-cyclopentyladenosine (**37**) (1.0 mmol), 2,2-dimethoxypropane (18.1 mmol), and camphorsulfonic acid (1.0 mmol) in anhydrous acetone (10 mL) was stirred at 55 °C for the time reported below. The solvent was removed in vacuo, and the residue was purified by column chromatography to afford the desired compounds.

2-Chloro-N^6-(±)-*endo*-norbornyl-9*H*-(2,3-*O*-isopropylidene-β-D-ribofuranosyl)adenine (17). The title compound was synthesized from **16** (reaction time 3 h). Chromatography on a silica gel column ($CHCl_3$−MeOH, 98:2) gave **17** as a white solid (80% yield). ^{1}H NMR (DMSO-d_6) δ 1.15−1.26 (m, 3H, norbornyl), 1.28, 1.50 (2s, 6H, CH_3), 1.35−1.44 (m, 3H, norbornyl), 1.58−1.63 (m, 1H, norbornyl), 1.81−1.93 (m, 1H, norbornyl), 2.16 (br s, 1H, norbornyl), 2.52 (s, 1H, norbornyl), 3.45−3.58 (m, 2H, H-5′), 4.17−4.22 (m, 1H, H-4′), 4.24 (br s, 1H, NHC*H*), 4.88−4.92 (m, 1H, H-3′), 5.06 (pseudo t, 1H, OH), 5.22−5.28 (m, 1H, H-2′), 6.05 (d, J = 2.6 Hz, 1H, H-1′), 8.32 (s, 1H, H-8), 8.38 (d, J = 6.4 Hz, 1H, NH). MS: *m*/*z* 436.9 $[M + H]^+$. Anal. ($C_{20}H_{26}ClN_5O_4$) C, H, N.

N^6-(±)-*endo*-Norbornyl-9*H*-(2-*C*-methyl-2,3-*O*-isopropylidene-β-D-ribofuranosyl)adenine (27). The title compound was synthesized from **23** (reaction time 7 h). Chromatography on a silica gel column ($CHCl_3$−MeOH, 99.5:0.5) gave **27** as a white solid (50% yield). ^{1}H NMR (DMSO-d_6) δ 1.10 (2s, 3H, CH_3), 1.20−1.31 (m, 3H, norbornyl), 1.35, 1.55 (2s, 6H, CH_3), 1.40−1.48 (m, 3H, norbornyl), 1.58−1.64 (m, 1H, norbornyl), 1.82−1.92 (m, 1H, norbornyl), 2.18 (br s, 1H, norbornyl), 2.52 (br s, 1H, norbornyl), 3.77 (dq, J = 6.4, 12.4 Hz, 2H, H-5′), 4.20−4.28 (m, 1H, H-4′), 4.35 (br s, 1H, NHC*H*), 4.58 (d, J = 2.1 Hz, 1H, H-3′), 5.40 (br s, 1H, OH), 6.22 (s, 1H, H-1′), 7.80 (d, J = 6.5 Hz, 1H, NH), 8.20 (s, 1H, H-2), 8.32 (s, 1H, H-8). MS: *m*/*z* 416.5 $[M + H]^+$. Anal. ($C_{21}H_{29}N_5O_4$) C, H, N.

2-Chloro-N^6-(±)-*endo*-norbornyl-9*H*-(2-*C*-methyl-2,3-*O*-isopropylidene-β-D-ribofuranosyl)adenine (28). The title compound was synthesized from **24** (reaction time 3 h) and purified by chromatography on a silica gel column ($CHCl_3$−MeOH, 99.5:0.5) as a white solid (95% yield). ^{1}H NMR (DMSO-d_6) δ 1.12 (2s, 3H, CH_3), 1.22−1.30 (m, 3H, norbornyl), 1.35, 1.55 (2s, 6H, CH_3), 1.40−1.48 (m, 3H, norbornyl), 1.58−1.64 (m, 1H, norbornyl), 1.82−1.92 (m, 1H, norbornyl), 2.16 (br s, 1H, norbornyl), 2.52 (br s, 1H, norbornyl), 3.65−3.75 (m, 2H, H-5′), 4.20−4.28 (m, 2H, NHC*H*, H-4′), 4.57 (d, J = 2.1 Hz, 1H, H-3′), 5.25 (t, J = 5.6 Hz, 1H, OH), 6.12 (s, 1H, H-1′), 8.36 (s, 1H, H-8), 8.42 (d, J = 6.8 Hz, 1H, NH). MS: *m*/*z* 450.9 $[M + H]^+$. Anal. ($C_{21}H_{28}ClN_5O_4$) C, H, N.

2-Chloro-N^6-cyclopentyl-9*H*-(2,3-*O*-isopropylidene-β-D-ribofuranosyl)adenine (38). The title compound was synthesized from **37** (reaction time 2 h). Chromatography on a silica gel column ($CHCl_3$−MeOH, 99:1) gave **38** as a white solid (75% yield). ^{1}H NMR (DMSO-d_6) δ 1.30, 1.50 (2s, 6H, CH_3), 1.44−1.60 (m, 4H, cyclopentyl), 1.62−1.72 (m, 2H, cyclopentyl), 1.82−1.98 (m, 2H,

cyclopentyl), 3.48−3.56 (m, 2H, H-5′), 4.20 (br s, 1H, H-4′), 4.38−4.46 (m, 1H, NHC*H*), 4.92 (dd, $J = 2.6$, 6.0 Hz, 1H, H-3′), 5.08 (pseudo t, 1H, OH), 5.26 (dd, $J = 3.0$, 6.0 Hz, 1H, H-2′), 6.04 (d, $J = 2.6$ Hz, 1H, H-1′), 8.35 (s, d, 2H, H-8 and NH). MS: *m*/*z* 410.8 $[M + H]^+$. Anal. ($C_{18}H_{24}ClN_5O_4$) C, H, N.

General Procedure for the Synthesis of Compounds 18, 29−32, and 39. Compounds **17**, **25**,[3a] **26**,[3a] **27**, **28**, or **38** (1.0 mmol) in dry acetonitrile (10 mL) under nitrogen atmosphere were stirred with cooling to −5 °C. $SOCl_2$ (3.0 mmol) was added portionwise followed by dry pyridine (2.0 mmol). After 30 min, the reaction mixture was stirred at room temperature. The procedure was repeated after 6 h, and the mixture was stirred at room temperature overnight. Water was added (5 mL), and the solution was neutralized with $NaHCO_3$ (1 M) and extracted with CH_2Cl_2 (3 × 10 mL). The organic layer was dried (Na_2SO_4), and the solvent was evaporated to dryness. The residue was purified by column chromatography as reported below.

2-Chloro-*N*^{6}-(±)-*endo*-norbornyl-9*H*-(2,3-*O*-isopropylidene-5-chloro-5-deoxy-β-D-ribofuranosyl)adenine (18). The title compound was synthesized from **17**. Chromatography on a silica gel column ($CHCl_3$) gave **18** as a white foam (70% yield). ^{1}H NMR (DMSO-d_6) δ 1.25−1.32 (m, 3H, norbornyl), 1.38, 1.55 (2s, 6H, CH_3), 1.36−1.43 (m, 3H, norbornyl), 1.55−1.62 (m, 1H, norbornyl), 1.88−1.95 (m, 1H, norbornyl), 2.18 (br s, 1H, norbornyl), 2.52 (s, 1H, norbornyl), 3.75 (dd, $J = 6.8$, 11.1 Hz, 1H, H-5′), 3.85 (dd, $J = 7.0$, 11.0 Hz, 1H, H-5′), 4.31−4.36 (m, 1H, H-4′), 4.39−4.44 (m, 1H, NHC*H*), 5.0 (dd, $J = 2.8$, 6.2 Hz, 1H, H-3′), 5.32 (dd, $J = 2.3$, 6.2 Hz, 1H, H-2′), 6.15 (d, $J = 2.1$ Hz, 1H, H-1′), 8.30 (s, 1H, H-8), 8.40 (d, $J = 7.3$ Hz, 1H, NH). MS: *m*/*z* 455.4 $[M + H]^+$. Anal. ($C_{20}H_{25}Cl_2N_5O_3$) C, H, N.

***N*^{6}-Cyclopentyl-9*H*-(2-*C*-methyl-2,3-*O*-isopropylidene-5-chloro-5-deoxy-β-D-ribofuranosyl)adenine (29).** The title compound was synthesized from **25**.[3a] Chromatography on a silica gel column ($CHCl_3$−MeOH, 99.5:0.5) gave **29** as a white foam (52% yield). ^{1}H NMR (DMSO-d_6) δ 1.20 (s, 3H, CH_3), 1.40, 1.55 (2s, 3H, CH_3), 1.52−1.62 (m, 4H, cyclopentyl), 1.62−1.72 (m, 2H, cyclopentyl), 1.86−1.98 (m, 2H, cyclopentyl), 4.07 (dq, $J = 6.4$, 11.1 Hz, 2H, H-5′), 4.36 (dt, $J = 3.1$, 6.3 Hz, 1H, H-4′), 4.43−4.52 (m, 1H, NHC*H*), 4.63 (d, $J = 3.0$ Hz, 1H, H-3′), 6.30 (s, 1H, H-1′), 7.80 (d, $J = 6.4$ Hz, 1H, NH), 8.20 (2s, 2H, H-2, H-8). MS: *m*/*z* 408.9 $[M + H]^+$. Anal. ($C_{19}H_{26}ClN_5O_3$) C, H, N.

2-Chloro-*N*^{6}-cyclopentyl-9*H*-(2-*C*-methyl-2,3-*O*-isopropylidene-5-chloro-5-deoxy-β-D-ribofuranosyl)adenine (30). The title compound was synthesized from **26**.[3a] Chromatography on a silica gel column ($CHCl_3$) gave **30** as a foam (50% yield). ^{1}H NMR (DMSO-d_6) δ 1.18 (s, 3H, CH_3), 1.40, 1.56 (2s, 6H, CH_3), 1.50−1.60 (m, 4H, cyclopentyl), 1.62−1.72 (m, 2H, cyclopentyl), 1.88−1.98 (m, 2H, cyclopentyl), 4.06 (dq, $J = 5.2$, 11.5 Hz, 2H, H-5′), 4.35 (q, $J = 7.3$ Hz, 1H, H-4′), 4.40−4.48 (m, 1H, NHC*H*), 4.60 (d, $J = 3.0$ Hz, 1H, H-3′), 6.20 (s, 1H, H-1′), 8.25 (s, 1H, H-8), 8.40 (d, $J = 7.7$ Hz, 1H, NH). MS: *m*/*z* 443.4 $[M + H]^+$. Anal. ($C_{19}H_{25}Cl_2N_5O_3$) C, H, N.

***N*^{6}-(±)-*endo*-Norbornyl-9*H*-(2-*C*-methyl-2,3-*O*-isopropylidene-5-chloro-5-deoxy-β-D-ribofuranosyl)-adenine (31).** The title compound was synthesized from **27**. Chromatography on a silica gel column ($CHCl_3$) gave **31** as a white solid (60% yield). ^{1}H NMR (DMSO-d_6) δ 1.20 (2s, 3H, CH_3), 1.23−1.32 (m, 3H, norbornyl), 1.35, 1.55 (2s, 6H, CH_3), 1.39−1.45 (m, 3H, norbornyl), 1.58−1.62 (m, 1H, norbornyl), 1.84−1.93 (m, 1H, norbornyl), 2.15 (br s, 1H, norbornyl), 2.52 (br s, 1H, norbornyl), 4.05 (dq, $J = 6.3$, 10.5 Hz, 2H, H-5′), 4.27−4.36 (m, 2H, NHC*H*, H-4′), 4.65 (d, $J = 2.6$ Hz, 1H, H-3′), 6.28 (s, 1H, H-1′), 7.85 (br s, 1H, NH), 8.20 (2s, 2H, H-2, H-8). MS: *m*/*z* 434.9 $[M + H]^+$. Anal. ($C_{21}H_{28}ClN_5O_3$) C, H, N.

2-Chloro-*N*^{6}-(±)-*endo*-norbornyl-9*H*-(2-*C*-methyl-2,3-*O*-isopropylidene-5-chloro-5-deoxy-β-D-ribofuranosyl)adenine (32). The title compound was synthesized from **28**. Chromatography on a silica gel column ($CHCl_3$) gave **32** as a white foam (69% yield). ^{1}H NMR (DMSO-d_6) δ 1.20 (s, 3H, CH_3), 1.25−1.32 (m, 3H, norbornyl), 1.40, 1.55 (2s, 6H, CH_3), 1.38−1.48 (m, 3H, norbornyl), 1.55−1.60 (m, 1H, norbornyl), 1.85−1.95 (m, 1H, norbornyl), 2.15 (br s, 1H, norbornyl), 2.52 (s, 1H, norbornyl), 4.05 (dq, $J = 6.4$, 10.7 Hz, 2H, H-5′), 4.20−4.28 (m, 1H, NHC*H*), 4.32−4.38 (m, 1H, H-4′), 4.60 (d, $J = 3.0$ Hz, 1H, H-3′), 6.20 (s, 1H, H-1′), 8.25 (s, 1H, H-8), 8.45 (d, $J = 6.8$ Hz, 1H, NH). MS: *m*/*z* 469.4 $[M + H]^+$. Anal. ($C_{21}H_{27}Cl_2N_5O_3$) C, H, N.

2-Chloro-*N*^{6}-cyclopentyl-9*H*-(2,3-*O*-isopropylidene-5-chloro-5-deoxy-β-D-ribofuranosyl)adenine (39). The title compound was synthesized from **38** and purified by chromatography on a silica gel column ($CHCl_3$) as a white solid (68% yield). ^{1}H NMR (DMSO-d_6): δ 1.33, 1.55 (2s, 6H, CH_3), 1.50−1.60 (m, 4H, cyclopentyl), 1.62−1.75 (m, 2H, cyclopentyl), 1.82−2.0 (m, 2H, cyclopentyl), 3.76 (dd, $J = 6.0$, 11.1 Hz, 1H, H-5′), 3.86 (dd, $J = 7.0$, 11.0 Hz, 1H, H-5′), 4.30−4.35 (m, 1H, H-4′), 4.36−4.46 (m, 1H, NHC*H*), 5.0 (dd, $J = 2.8$, 6.2 Hz, 1H, H-3′), 5.36 (dd, $J = 2.3$, 6.2 Hz, 1H, H-2′), 6.16 (d, $J = 2.1$ Hz, 1H, H-1′), 8.32 (s, 1H, H-8), 8.40 (d, $J = 7.3$ Hz, 1H, NH). MS: *m*/*z* 429.4 $[M + H]^+$. Anal. ($C_{18}H_{23}Cl_2N_5O_3$) C, H, N.

General Procedure for the Synthesis of Compounds 33−36 and 40. To an ice cooled solution of 2-fluorothiophenol (4.74 mmol) in dry DMF (10 mL), under nitrogen atmosphere, was added NaH 60% (3.84 mmol) in mineral oil portionwise. When the development of H_2 was complete, compounds **29**−**32** or **39** (1.0 mmol) were added and the mixture was stirred at room temperature for the time reported below. The solvent was removed in vacuo, and the residue was purified by column chromatography.

***N*^{6}-Cyclopentyl-9*H*-[2-*C*-methyl-2,3-*O*-isopropylidene-5-deoxy-5-(2-fluorophenylthio)-β-D-ribofuranosyl]adenine (33).** The title compound was synthesized from **29** (reaction time 6 h). Chromatography on a silica gel column ($CHCl_3$−MeOH, 99.5:0.5) gave **33** as a foam (91% yield). ^{1}H NMR (DMSO-d_6) δ 1.15 (s, 3H, CH_3), 1.35, 1.50 (2s, 6H, CH_3), 1.50−1.62 (m, 4H, cyclopentyl), 1.65−1.75 (m, 2H, cyclopentyl), 1.86−1.98 (m, 2H, cyclopentyl), 3.48 (d, $J = 6.4$ Hz, 2H, H-5′), 4.25 (dt, $J = 3.0$, 6.6 Hz, 1H, H-4′), 4.42−4.54 (m, 1H, NHC*H*), 4.60 (d, $J = 3.0$ Hz, 1H, H-3′), 6.20 (s, 1H, H-1′), 7.15−7.32 (m, 3H, arom.), 7.53 (t, $J = 6.4$ Hz, 1H, arom.), 7.80 (d, $J = 7.0$ Hz, 1H, NH), 8.10 (s, 1H, H-2), 8.20 (s, 1H, H-8). MS: *m*/*z* 500.9 $[M + H]^+$. Anal. ($C_{25}H_{30}FN_5O_3S$) C, H, N.

2-Chloro-*N*^{6}-cyclopentyl-9*H*-[2-*C*-methyl-2,3-*O*-isopropylidene-5-deoxy-5-(2-fluorophenylthio)-β-D-ribofuranosyl]adenine (34). The title compound was synthesized from **30** (reaction time 8 h). Chromatography on a silica gel column ($CHCl_3$) gave **34** as an oil (91% yield). ^{1}H NMR (DMSO-d_6) δ 1.16 (s, 3H, CH_3), 1.35, 1.48 (2s, 6H, CH_3), 1.50−1.62 (m, 4H, cyclopentyl), 1.64−1.75 (m, 2H, cyclopentyl), 1.85−2.0 (m, 2H, cyclopentyl), 3.46 (d, $J = 6.8$ Hz, 2H, H-5′), 4.18−4.22 (m, 1H, H-4′), 4.38−4.45 (m, 1H, NHC*H*), 4.60 (d, $J = 3.0$ Hz, 1H, H-3′), 6.12 (s, 1H, H-1′), 7.15−7.30 (m, 3H, arom.), 7.52 (t, $J = 7.3$ Hz, 1H, arom.), 8.10 (s, 1H, H-8), 8.40 (d, $J = 7.7$ Hz, 1H, NH). MS: *m*/*z* 535.1 $[M + H]^+$. Anal. ($C_{25}H_{29}ClFN_5O_3S$) C, H, N.

***N*^{6}-(±)-*endo*-Norbornyl-9*H*-[2-*C*-methyl-2,3-*O*-isopropylidene-5-deoxy-5-(2-fluorophenylthio)-β-D-ribofuranosyl]adenine (35).** The title compound was synthesized from **31** (reaction time 6 h). Chromatography on a silica gel column ($CHCl_3$) gave **35** as a white solid (58% yield). ^{1}H NMR (DMSO-d_6) δ 1.15 (s, 3H, CH_3), 1.25 (m, 3H, norbornyl), 1.35, 1.50 (2s, 6H, CH_3), 1.39−1.48 (m, 3H, norbornyl), 1.57−1.64 (m, 1H, norbornyl), 1.83−1.94 (m, 1H, norbornyl), 2.16 (br s, 1H, norbornyl), 2.52 (br s, 1H, norbornyl), 3.50 (d, $J = 6.8$ Hz, 2H, H-5′), 4.18−4.23 (m, 1H, H-4′), 4.31−4.38 (m, 1H, NHC*H*), 4.65 (br s, 1H, H-3′), 6.20 (s, 1H, H-1′), 7.15−7.30 (m, 3H, arom.), 7.51−7.58 (m, 1H, arom.), 7.85 (d, $J = 6.8$ Hz, 1H, NH), 8.10 (s, 1H, H-2), 8.20 (s, 1H, H-8). MS: *m*/*z* 526.6 $[M + H]^+$. Anal. ($C_{27}H_{32}FN_5O_3S$) C, H, N.

2-Chloro-*N*^{6}-(±)-*endo*-norbornyl-9*H*-[2-*C*-methyl-2,3-*O*-isopropylidene-5-deoxy-5-(2-fluorophenylthio)-β-D-ribofuranosyl]-adenine (36). The compound was synthesized from **32** (reaction time 7 h) and purified by chromatography on a silica gel column ($CHCl_3$−MeOH, 99.5:0.5) as a white foam (81% yield). ^{1}H NMR (DMSO-d_6) δ 1.15 (2s, 3H, CH_3), 1.22−1.30 (m, 3H, norbornyl), 1.35, 1.50 (2s, 6H, CH_3), 1.40−1.48 (m, 3H, norbornyl), 1.52−1.66 (2m, 1H, norbornyl), 1.82−1.98 (2m, 1H, norbornyl), 2.15 (br s,

1H, norbornyl), 2.52 (br s, 1H, norbornyl), 3.46 (d, J = 6.8 Hz, 2H, H-5′), 4.18−4.28 (m, 2H, NHC*H*, H-4′), 4.60 (br s, 1H, H-3′), 6.12 (s, 1H, H-1′), 7.12−7.32 (m, 3H, arom.), 7.52 (t, J = 7.7 Hz, 1H, arom.), 8.13 (2s, 1H, H-8), 8.45 (d, J = 6.4 Hz, 1H, NH). MS: m/z 561.1 $[M + H]^+$. Anal. ($C_{27}H_{31}ClFN_5O_3S$) C, H, N.

2-Chloro-N^6-cyclopentyl-9*H*-[2,3-*O*-isopropylidene-5-deoxy-5-(2-fluorophenylthio)-β-D-ribofuranosyl]adenine (40). The title compound was synthesized from **39** (reaction time 5 h) and purified by chromatography on a silica gel column (CH_3Cl−MeOH, 99.5:0.5) as a white foam (95% yield). ^{1}H NMR (DMSO-d_6) δ 1.30, 1.45 (2s, 6H, CH_3), 1.50−1.60 (m, 4H, cyclopentyl), 1.62−1.72 (m, 2H, cyclopentyl), 1.86−1.98 (m, 2H, cyclopentyl), 3.25 (d, J = 6.8 Hz, 2H, H-5′), 4.25 (dt, J = 2.6, 7.0 Hz, 1H, H-4′), 4.36−4.40 (m, 1H, NHC*H*), 5.0 (dd, J = 2.8, 6.2 Hz, 1H, H-3′), 5.48 (dd, J = 2.1, 6.4 Hz, 1H, H-2′), 6.20 (d, J = 1.7 Hz, 1H, H-1′), 7.10−7.28 (m, 3H, arom.), 7.45 (t, J = 7.3 Hz, 1H, arom.), 8.33 (s, 1H, H-8), 8.38 (d, J = 7.3 Hz, 1H, NH). MS: m/z 521.1 $[M + H]^+$. Anal. ($C_{24}H_{27}ClFN_5O_3S$) C, H, N.

General Procedure for the Synthesis of Compounds 4−8 and 10−14. Compounds **18**, **29**−**36**, and **40** (1.0 mmol) were treated with HCOOH 70% in water (10 mL), and the mixture was stirred at 40 °C for the time reported below. The solvent was evaporated in vacuo, and the residue was coevaporated several times with CH_3OH and then purified by column chromatography.

2-Chloro-N^6-(±)-*endo*-norbornyl-9*H*-(5-chloro-5-deoxy-β-D-ribofuranosyl)adenine (4). The title compound was synthesized from **18** (reaction time 6 h). Chromatography on a silica gel column ($CHCl_3$−MeOH, 98:2) gave **4** as a white foam (60% yield). ^{1}H NMR (DMSO-d_6) δ 1.21−1.30 (m, 3H, norbornyl), 1.33−1.45 (m, 3H, norbornyl), 1.50−1.65 (2m, 1H, norbornyl), 1.83−1.96 (2m, 1H, norbornyl), 2.16 (br s, 1H, norbornyl), 2.52 (br s, 1H, norbornyl), 3.81−3.88 (m, 1H, H-5′), 3.90−3.96 (m, 1H, H-5′), 4.08 (q, J = 5.6 Hz, 1H, H-4′), 4.14−4.18 (m, 1H, H-3′), 4.21−4.27 (m, 1H, NHC*H*), 4.61−4.66 (m, 1H, H-2′), 5.48 (d, J = 5.1 Hz, 1H, OH), 5.62 (d, J = 6.0 Hz, 1H, OH), 5.85 (d, J = 6.0 Hz, 1H, H-1′), 8.37 (s, 1H, H-8), 8.40 (d, J = 6.8 Hz, 1H, NH). MS: m/z 415.3 $[M + H]^+$. Anal. ($C_{17}H_{21}Cl_2N_5O_3$) C, H, N.

***N*^{6}-Cyclopentyl-9*H*-(2-*C*-methyl-5-chloro-5-deoxy-β-D-ribofuranosyl)adenine (5).** The title compound was synthesized from **29** (reaction time 6 h). Chromatography on a silica gel column ($CHCl_3$−MeOH, 99:1) gave **5** as a white foam (60% yield). ^{1}H NMR ($CDCl_3$) δ 1.05 (s, 3H, CH_3), 1.52−1.82 (m, 6H, cyclopentyl), 2.12−2.18 (m, 2H, cyclopentyl), 3.88 (dd, J = 4.9, 11.7 Hz, 1H, H-5′), 3.94 (dd, J = 4.7, 11.0 Hz, 1H, H-5′), 4.15 (br s, 1H, H-4′), 4.35 (q, J = 5.1 Hz, 1H, H-3′), 4.57−4.62 (m, 1H, NHC*H*), 5.60 (br s, 1H, OH), 5.85 (br s, 1H, OH), 6.0 (s, 1H, H-1′), 8.0 (br s, 2H, H-2, NH), 8.38 (s, 1H, H-8). MS: m/z 368.8 $[M + H]^+$. Anal. ($C_{16}H_{22}ClN_5O_3$) C, H, N.

2-Chloro-N^6-cyclopentyl-9*H*-(2-*C*-methyl-5-chloro-5-deoxy-β-D-ribofuranosyl)adenine (6). The title compound was synthesized from **30** (reaction time 12 h). Chromatography on a silica gel column (CH_3Cl−MeOH, 99:1) gave **6** as a white foam (70% yield). ^{1}H NMR (DMSO-d_6) δ 0.80 (s, 3H, CH_3), 1.47−1.52 (m, 4H, cyclopentyl), 1.66−1.74 (m, 2H, cyclopentyl), 1.83−1.97 (m, 2H, cyclopentyl), 3.98−4.10 (m, 4H, H-5′, H-4′, H-3′), 4.37−4.43 (m, 1H, NHC*H*), 5.40 (s, 1H, OH), 5.52 (d, J = 6.4 Hz, 1H, OH), 5.90 (s, 1H, H-1′), 8.24 (s, 1H, H-8), 8.35 (d, J = 6.8 Hz, 1H, NH). MS: m/z 403.3 $[M + H]^+$. Anal. ($C_{16}H_{21}Cl_2N_5O_3$) C, H, N.

***N*^{6}-(±)-*endo*-Norbornyl-9*H*-(2-*C*-methyl-5-chloro-5-deoxy-β-D-ribofuranosyl)adenine (7).** The title compound was synthesized from **31** (reaction time 10 h). Chromatography on a silica gel column (CH_3Cl−MeOH 98:2) gave **7** as a white solid (67% yield). ^{1}H NMR (DMSO-d_6) δ 0.80 (s, 3H, CH_3), 1.21−1.29 (m, 3H, norbornyl), 1.39−1.45 (m, 3H, norbornyl), 1.57−1.64 (m, 1H, norbornyl), 1.83−1.95 (m, 1H, norbornyl), 2.16 (br s, 1H, norbornyl), 2.52 (br s, 1H, norbornyl), 3.96−4.04 (m, 2H, H-5′), 4.06−4.11 (m, 1H, H-4′), 4.12−4.18 (m, 1H, H-3′), 4.31−4.39 (m, 1H, NHC*H*), 5.35 (s, 1H, OH), 5.48 (d, J = 6.4 Hz, 1H, OH), 5.98 (s, 1H, H-1′), 7.80 (br s, 1H, NH), 8.20 (s, 1H, H-2), 8.22 (s, 1H, H-8). MS: m/z 394.9 $[M + H]^+$. Anal. ($C_{18}H_{24}ClN_5O_3$) C, H, N.

2-Chloro-N^6-(±)-*endo*-norbornyl-9*H*-(2-*C*-methyl-5-chloro-5-deoxy-β-D-ribofuranosyl)adenine (8). The title compound was synthesized from **32** (reaction time 7 h). Chromatography on a silica gel column (CH_3Cl−MeOH, 99:1) gave **8** as a white solid (81% yield). ^{1}H NMR (DMSO-d_6) δ 0.80 (s, 3H, CH_3), 1.22−1.27 (m, 3H, norbornyl), 1.39−1.44 (m, 3H, norbornyl), 1.56−1.64 (2m, 1H, norbornyl), 1.92−1.95 (2m, 1H, norbornyl), 2.16 (br s, 1H, norbornyl), 2.52 (br s, 1H, norbornyl), 3.97−4.09 (m, 4H, H-5′, H-4′, H-3′), 4.25 (br s, 1H, NHC*H*), 5.40 (s, 1H, OH), 5.50 (d, J = 6.0 Hz, 1H, OH), 5.90 (s, 1H, H-1′), 8.28 (s, 1H, H-8), 8.40 (d, J = 6.4 Hz, 1H, NH). MS: m/z 429.3 $[M + H]^+$. Anal. ($C_{18}H_{23}Cl_2N_5O_3$) C, H, N.

2-Chloro-N^6-cyclopentyl-9*H*-[5-deoxy-5-(2-fluorophenylthio)-β-D-ribofuranosyl]adenine (10). The title compound was synthesized from **40** (reaction time 7 h). Chromatography on a silica gel column ($CHCl_3$−MeOH, 99.5:0.5) gave **10** as a white foam (64% yield). ^{1}H NMR (DMSO-d_6) δ 1.50−1.60 (m, 4H, cyclopentyl), 1.62−1.72 (m, 2H, cyclopentyl), 1.88−2.0 (m, 2H, cyclopentyl), 3.30 (dd, J = 7.3, 13.7 Hz, 1H, H-5′), 3.40 (dd, J = 5.8, 13.9 Hz, 1H, H-5′), 3.95−4.05 (m, 1H, H-4′), 4.14 (q, J = 4.9 Hz, 1H, H-3′), 4.35−4.45 (m, 1H, NHC*H*), 4.72 (q, J = 6.0 Hz, 1H, H-2′), 5.42 (d, J = 3.7 Hz, 1H, OH), 5.56 (d, J = 6.0 Hz, 1H, OH), 5.80 (d, J = 6.0 Hz, 1H, H-1′), 7.10−7.26 (m, 3H, arom.), 7.45 (t, J = 7.9 Hz, 1H, arom.), 8.32 (s and d, 2H, H-8, NH). MS: m/z 481.0 $[M + H]^+$. Anal. ($C_{21}H_{23}ClFN_5O_3S$) C, H, N.

***N*^{6}-Cyclopentyl-9*H*-[2-*C*-methyl-5-deoxy-5-(2-fluorophenylthio)-β-D-ribofuranosyl]adenine (11).** The title compound was synthesized from **33** (reaction time 17 h). Chromatography on a silica gel column ($CHCl_3$−MeOH, 99.5:0.5) gave **11** as a white solid (82% yield). ^{1}H NMR (DMSO-d_6) δ 0.80 (s, 3H, CH_3), 1.50−1.62 (m, 4H, cyclopentyl), 1.64−1.76 (m, 2H, cyclopentyl), 1.82−1.98 (m, 2H, cyclopentyl), 3.45 (d, J = 5.6 Hz, 2H, H-5′), 4.05 (dt, J = 1.5, 5.6 Hz, 1H, H-4′), 4.12−4.18 (m, 1H, H-3′), 4.44−4.54 (m, 1H, NHC*H*), 5.30 (s, 1H, OH), 5.48 (d, J = 6.0 Hz, 1H, OH), 5.90 (s, 1H, H-1′), 7.10−7.26 (m, 3H, arom.), 7.46 (t, J = 7.7 Hz, 1H, arom.), 7.76 (d, J = 6.8 Hz, 1H, NH), 8.20 (s, 1H, H-2), 8.24 (s, 1H, H-8). MS: m/z 460.6 $[M + H]^+$. Anal. ($C_{22}H_{26}FN_5O_3S$) C, H, N.

2-Chloro-N^6-cyclopentyl-9*H*-[2-*C*-methyl-5-deoxy-5-(2-fluorophenylthio)-β-D-ribofuranosyl]adenine (12). The title compound was synthesized from **34** (reaction time 9 h). Chromatography on a silica gel column ($CHCl_3$−MeOH, 99.5:0.5) gave **12** as a white solid (58% yield). ^{1}H NMR (DMSO-d_6) δ 0.80 (s, 3H, CH_3), 1.46−1.61 (m, 4H, cyclopentyl), 1.62−1.73 (m, 2H, cyclopentyl), 1.83−1.97 (m, 2H, cyclopentyl), 3.42−3.52 (m, 2H, H-5′), 4.0 (dt, J = 3.7, 8.7 Hz, 1H, H-4′), 4.07−4.12 (m, 1H, H-3′), 4.37−4.42 (m, 1H, NHC*H*), 5.35 (br s, 1H, OH), 5.50 (d, J = 6.4 Hz, 1H, OH), 5.85 (s, 1H, H-1′), 7.10 (t, J = 7.3 Hz, 1H, arom.), 7.17−7.23 (m, 2H, arom.), 7.45 (t, J = 7.7 Hz, 1H, arom.), 8.25 (s, 1H, H-8), 8.38 (d, J = 7.3 Hz, 1H, NH). MS: m/z 495.0 $[M + H]^+$. Anal. ($C_{22}H_{25}ClFN_5O_3S$) C, H, N.

***N*^{6}-(±)-*endo*-Norbornyl-9*H*-[2-*C*-methyl-5-deoxy-5-(2-fluorophenylthio)-β-D-ribofuranosyl]adenine (13).** The title compound was synthesized from **35** (reaction time 6 h). Chromatography on a silica gel column ($CHCl_3$−MeOH, 99.5:0.5) gave **13** as a white solid (60% yield). ^{1}H NMR (DMSO-d_6) δ 0.80 (s, 3H, CH_3), 1.19−1.27 (m, 3H, norbornyl), 1.38−1.43 (m, 3H, norbornyl), 1.56−1.62 (m, 1H, norbornyl), 1.83−1.92 (m, 1H, norbornyl), 2.15 (br s, 1H, norbornyl), 2.52 (br s, 1H, norbornyl), 3.50 (d, J = 6.8 Hz, 2H, H-5′), 3.97−4.03 (m, 1H, H-4′), 4.13−4.21 (m, 1H, H-3′), 4.31−4.39 (m, 1H, NHC*H*), 5.30 (s, 1H, OH), 5.45 (d, J = 6.8 Hz, 1H, OH), 5.93 (s, 1H, H-1′), 7.12 (t, J = 7.3 Hz, 1H, arom.), 7.18−7.26 (m, 2H, arom.), 7.45 (t, J = 7.7 Hz, 1H, arom.), 7.82 (d, J = 6.7 Hz, NH), 8.20 (s, 1H, H-2), 8.25 (s, 1H, H-8). MS: m/z 486.6 $[M + H]^+$. Anal. ($C_{24}H_{28}FN_5O_3S$) C, H, N.

2-Chloro-N^6-(±)-*endo*-norbornyl-9*H*-[2-*C*-methyl-5-deoxy-5-(2-fluorophenylthio)-β-D-ribofuranosyl]adenine (14). The title compound was synthesized from **36** (reaction time 13 h). Chromatography on a silica gel column (CH_3Cl−MeOH, 99.5:0.5) gave **14** as a white solid (75% yield). ^{1}H NMR (DMSO-d_6) δ 0.80 (s, 3H, CH_3), 1.22−1.28 (m, 3H, norbornyl), 1.32−1.44 (m, 3H,

norbornyl), 1.52−1.68 (2m, 1H, norbornyl), 1.84−1.98 (2m, 1H, norbornyl), 2.15 (br s, 1H, norbornyl), 2.52 (br s, 1H, norbornyl), 3.42−3.50 (m, 2H, H-5′), 3.38−4.02 (m, 1H, H-4′), 4.04−4.12 (m, 1H, H-3′), 4.22 (br s, 1H, NHC*H*), 5.33 (s, 1H, OH), 5.50 (d, J = 6.8 Hz, 1H, OH), 5.85 (s, 1H, H-1′), 7.12 (t, J = 7.3 Hz, 1H, arom.), 7.20−7.28 (m, 3H, arom.), 7.45 (t, J = 7.7 Hz, 1H, arom.), 8.25 (s, 1H, H-8), 8.42 (d, J = 6.4 Hz, 1H, NH). MS: *m*/*z* 521.1 $[M + H]^+$. Anal. ($C_{24}H_{27}ClFN_5O_3S$) C, H, N.

Computational Chemistry. Molecular modeling and graphics manipulations were performed using the molecular operating environment (MOE)[31] and UCSF-CHIMERA software packages,[32] running on a 2 CPU (PIV 2.0−3.0 GHZ) Linux workstation. Energy minimizations and MD simulations were realized by employing the AMBER 9 program,[33] selecting the Cornell et al. force field.[34]

Residue Indexing. The convention used for the amino acid identifiers, according to the approach of Ballesteros and Weinstein,[35] facilitates comparison of aligned residues within the family of Group A GPCRs. To the most conserved residue in a given TM (TMX, where X is the TM number) is assigned the number X.50, and residues within a given TM are then indexed relative to the 50 position.

Construction of the hA_1 AR and hA_3 AR Homology Models. The structural models of hA_1 AR and hA_3 AR were built using the recently reported 2.8 Å crystal structure of b-Rho (PDB entry code 1F88) as a structural template.[13] We modeled only the TM domains, since the function of the loops has still not been defined. Although site-directed mutagenesis suggests a role for AR loops, and in particular for the second extracellular (E2) ones, it remains unclear whether the E2 loop is in direct contact with ligands or whether it contributes to the overall physical architecture of the receptor protein.[36] Briefly, the hA_1 AR and hA_3 AR sequences were retrieved from the SWISS-PROT database[37] and aligned with the sequence of b-Rho using CLUSTALW software[38] with the following settings: matrix = Blosum series; gap opening penalty = 10; gap extension penalty = 0.05. Afterward, we checked and, where necessary, manually corrected this alignment to reflect the known alignment features of class A GPCRs, such as the highly conserved positions and gap-free TM regions. In particular, the alignment was guided by the highly conserved amino acid residues, including the D/ERY motif (D/E3.49, R3.50, and Y3.51), the two proline residues P4.50 and P6.50, and the NPXXY motif in TM7 (N7.49, P7.50, and Y7.53).[39] Extension of each helix was contemplated by taking into account the experimental length of the b-Rho helices and the secondary structure prediction of both hA_1 AR and hA_3 AR obtained with the PSIPRED software,[40] as well as the sequence conservation in the possible extensions of the helices. Individual TM helical segments were built as ideal helices (using ϕ and Ψ angles of −63.0° and −41.6°, respectively) with side chains placed in prevalent rotamers and representative proline kink geometries. Each model helix was capped with an acetyl group at the *N*-terminus and a *N*-methyl group at the *C*-terminus. These structures were then grouped by adding one at a time until a helical bundle (TM region), matching the overall characteristics of the crystallographic structure of b-Rho, was obtained. The hA_1 AR and hA_3 AR helical bundles were subjected to a preliminary minimization and 200 ps of MD, after which the final structures were minimized. When MD simulations are carried out in the gas phases, skipping the explicit environment requires the use of a set of restraints, to replace the natural stabilizing effects of the membrane bilayer on the TM domains. Accordingly, restraints with a force constant of 10 kcal mol^{-1} $Å^{-2}$ were applied to backbone for the first 100 ps, and for the remaining 100 ps, these restraints were reduced to 1 kcal mol^{-1} $Å^{-2}$. The options of MD at 300 K with a 0.2 ps coupling constant were a time step of 1 fs and a nonbonded update every 25 fs. The lengths of bonds with hydrogen atoms were constrained according to the SHAKE algorithm.[41] The average structure from the last 50 ps trajectory of MD was reminimized with backbone constraints in the secondary structure.

Definition of the Rotameric State of χ_1. Different nomenclatures have been used to define the rotameric state of side chain torsion angles. The nomenclature employed here for the χ_1 torsion angle is that described by Shi et al.[27] When the heavy atom at the γ position is at a position opposite to the backbone nitrogen when viewed from the β-carbon to the α-carbon, the χ_1 is defined to be *trans*. When the heavy atom at the χ_1 position is at a position opposite to the backbone carbon when viewed from the β-carbon to the α-carbon, the χ_1 is defined to be *gauche*$^+$. When the heavy atom at the γ position is at a position opposite to the α-hydrogen when viewed from the β-carbon to the α-carbon, the χ_1 is defined to be *gauche*$^-$. The stabilities of three different χ_1 angles of W6.48 set at 60°, 180°, and −60° were compared. A minimized *gauche*$^+$ conformation with a χ_1 angle of −98° in the ground-state had the lowest energy among three different geometries. A *gauche*$^-$ conformer of W6.48 with the highest energy seemed to be similar to the Meta I state conformation, because it displayed the most outward anticlockwise rotation from the extracellular view, as b-Rho studies suggested. This putative Meta I state of hA_1 AR and hA_3 AR was used for agonist docking.

Docking Simulations. The core structures of compounds CPA, (±)-ENBA, **1**, and **3** were retrieved from the Cambridge Structural Database (CSD)[42] and modified using standard bond lengths and bond angles of the MOE fragment library. Since Trivedi et al.[4a] reported that the 1*R*,2*S*,4*S* isomer of the N^6-(2-*endo*-norbornyl) system of (±)-ENBA was more potent than the 1*S*,2*R*,4*R* one at the rat A_1 AR, we considered only the 1*R*,2*S*,4*S* isomer of (±)-ENBA and **3** for docking calculations. Geometry optimizations of compounds were accomplished with the MMFF94 force field,[43] available within MOE. CPA, chosen as a reference compound, was manually docked into both hA_1 AR and hA_3 AR binding sites, bearing in mind the known mutagenesis data. As regards hA_1 AR, CPA was docked in such a manner as to give H-bonds with T91 (3.36),[25] N254 (6.55), T277 (7.42),[44] and H278 (7.43)[45] and a lipophilic interaction (through the cyclopentyl moiety) with L88 (3.33),[25] in accordance with the main mutagenesis data and our previous computational studies.[3a,4b] In the case of hA_3 AR, CPA was manually introduced into the binding site, considering the interactions with T94 (3.36),[28] N250 (6.55),[25] and H272 (7.43),[23,46] suggested by mutagenesis data. Compounds **1** and **3** present the adenine group as their central core, and their initial docking position into both hA_1 AR and hA_3 AR binding sites was obtained by superimposing this group on that of the final structure of CPA in either hA_1 AR and hA_3 AR, respectively. In this position, the two ligands exhibited the interactions suggested by mutagenesis data.

Molecular Dynamics Simulations. Refinement of the ligand/receptor complexes was achieved by in vacuo energy minimization with the SANDER module of AMBER, applying an energy penalty force constant of 10 kcal·mol^{-1}·$Å^{-2}$ on the protein backbone atoms. The geometry-optimized complexes were then used as the starting point for subsequent 1 ns MD simulation, during which the protein backbone atoms were constrained by means of decreasing force constants; moreover, also the main ligand/receptor interactions were restrained. More specifically, an initial restraint with a force constant of 10 kcal·mol^{-1}·$Å^{-2}$ was applied on all the α carbons; this force constant decreased during the whole MD, and in the last 200 ps, its value was 0.1 kcal·mol^{-1}·$Å^{-2}$. As regards the main ligand/receptor interactions, a restraint of 50 kcal·mol^{-1}·$Å^{-2}$ was applied for 700 ps of MD simulation and, in the last 300 ps, the restraint was removed. General AMBER force field (GAFF) parameters were assigned to ligands, while the partial charges were calculated using the AM1-BCC method as implemented in the ANTECHAMBER suite of AMBER. A time step of 1 fs and a nonbonded pairlist updated every 25 fs were used for the MD simulations. The temperature was regulated by way of Langevin dynamics, with a collision frequency γ = 1.0 ps^{-1}. An average structure was calculated from the last 200 ps trajectory and energy-minimized using the steepest descent and conjugate gradient methods as specified above. RMSDs from the initial structures and interatomic distances were monitored using the PTRAJ module in AMBER.

Binding Assay and Adenylyl Cyclase Assay at Cloned Human Adenosine Receptors. K_i-values were determined in competition experiments with membranes from CHO cells stably transfected with the individual human adenosine receptor sub-

types.[11] For A_1 AR 1 nM [^{3}H]CCPA was used as a radioligand, [^{3}H]NECA was used for the A_{2A} (30 nM), and [^{3}H]HEMADO was used for the A_3 (1 nM) subtype. In the case of the A_{2B} receptor, K_i values were calculated from IC_{50} values determined by inhibition of NECA-stimulated adenylyl cyclase activity.[11] All binding data were calculated by nonlinear curve fitting with the program SCTFIT.[47] The functional activity of selected derivatives at the A_1 receptor was determined in adenylyl cyclase experiments. The inhibition of forskolin-stimulated adenylyl cyclase via A_1 and A_3 receptors was measured as described earlier.[12,48]

Formalin Test. The experimental procedures applied in the formalin test were approved by the Animal Ethics Committee of the Second University of Naples. Animal care was in compliance with the IASP and European Community guidelines on the use and protection of animals in experimental research (E.C. L358/118/12/86). All efforts were made to minimize animal suffering and to reduce the number of animals used. Formalin injection induces a biphasic stereotypical nocifensive behavior.[29] Nociceptive responses are divided into an early, short lasting first phase (0−7 min) caused by a primary afferent discharge produced by the stimulus, followed by a quiescent period and then a second, prolonged phase (15−60 min) of tonic pain. Mice received formalin (1.25% in saline, 30 μL) in the dorsal surface of one side of the hind-paw. Each mouse was randomly assigned to one of the experimental groups (n = 8−10) and placed in a Plexiglas cage and allowed to move freely for 15−20 min. A mirror was placed at a 45° angle under the cage to allow full view of the hind-paws. Lifting, favoring, licking, shaking, and flinching of the injected paw were recorded as nociceptive responses. The total time of the nociceptive response was measured every 5 min and expressed as the total time of the nociceptive responses in minutes (mean ± SEM). Recording of nociceptive behavior commenced immediately after formalin injection and was continued for 60 min. The version of the formalin test we applied is based on the fact that a correlational analysis showed that no single behavioral measure can be a strong predictor of formalin or drug concentrations on spontaneous behaviors.[49] Consistently, we considered that a simple sum of time spent licking plus elevating the paw, or the weighted pain score, is in fact superior to any single (lifting, favoring, licking, shaking, and flinching) measure (r ranging from 0.75 to 0.86).[50] Treatments: groups of 8−10 animals per treatment were used with each animal being used for one treatment only. Mice received intraperitoneal vehicle (10% DMSO in 0.9% NaCl) or different doses of (±)-ENBA, 5′Cl5′d-(±)-ENBA, or DPCPX.

Acknowledgment. This project was supported by a grant from University of Camerino and by the Italian MIUR funds. The work was presented in part at the Purines 2008 Meeting (Copenhangen, Denmark, 2008). We thank M. Brandi, F. Lupidi, G. Rafaiani, and M. Ricciutelli for technical assistance.

Supporting Information Available: Method for the synthesis of compounds **1**, **9**, and **41** (Scheme 4); analytical data of all synthesized compounds; binding affinity with confidence intervals (Table S1); Ramachandran plots of the hA_1 AR and hA_3 AR models (Figures S1 and S2); plots showing the time dependence of the positional rmsd of backbone atoms and the total energy over the course of the 1 ns trajectory in the hA_1 AR and hA_3 AR, respectively, complexed with CPA (Figures S3a and S5a), (±)-ENBA (Figures S3b and S5b), **1** (Figures S4a and S6a), and **3** (Figures S4b and S6b). This material is available free of charge *via* the Internet at http://pubs.acs.org.

References

(1) Gao, Z.-G.; Jacobson, K. A. Emerging adenosine receptor agonists. *Expert Opin. Emerging Drugs* **2007**, *12*, 479–492.

(2) Dhalla, A. K.; Shryock, J. C.; Shreeniwas, R.; Belardinelli, L. Pharmacology and therapeutic applications of A_1 adenosine receptor ligands. *Curr. Top. Med. Chem.* **2003**, *3*, 369–385.

(3) (a) Cappellacci, L.; Franchetti, P.; Vita, P.; Petrelli, R.; Lavecchia, A.; Costa, B.; Spinetti, F.; Martini, C.; Klotz, K.-N.; Grifantini, M. 5′-Carbamoyl derivatives of 2′-*C*-methyl-purine nucleosides as selective A_1 adenosine receptor agonists: Affinity, efficacy, and selectivity for A_1 receptor from different species. *Bioorg. Med. Chem.* **2008**, *16*, 336–353. (b) Ashton, T. D.; Baker, S. P.; Hutchinson, S. A.; Scammells, P. J. N6-substituted C5′-modified adenosines as A_1 adenosine receptor agonists. *Bioorg. Med. Chem.* **2008**, *16*, 1861−1873, and references reported therein.

(4) (a) Trivedi, B. K.; Bridges, A. J.; Patt, W. C.; Priebe, S. R.; Bruns, R. F. N6-Bicycloalkyladenosines with unusually high potency and selectivity for the adenosine A_1 receptor. *J. Med. Chem.* **1989**, *32*, 8–11. (b) Cappellacci, L.; Franchetti, P.; Pasqualini, M.; Petrelli, R.; Vita, P.; Lavecchia, A.; Novellino, E.; Costa, B.; Martini, C.; Klotz, K.-N.; Grifantini, M. Synthesis, biological evaluation, and molecular modeling of ribose-modified adenosine analogues as adenosine receptor agonists. *J. Med. Chem.* **2005**, *48*, 1550–1562. (c) Elzein, E.; Kalla, R.; Li, X.; Perry, T.; Marquart, T.; Micklatcher, M.; Li, Y.; Wu, Y.; Zeng, D.; Zablocki, J. A. N6-Cycloalkyl-2-substituted adenosine derivatives as selective, high affinity adenosine A_1 receptor agonists. *Bioorg. Med. Chem. Lett.* **2007**, *17*, 161–166.

(5) (a) van der Wenden, E. M.; Carnielli, M.; Roelen, H. C.; Lorenzen, A.; von Frijtag Drabbe Kunzel, J. K.; Ijzerman, A. P. 5′-Substituted adenosine analogs as new high-affinity partial agonists for the adenosine A_1 receptor. *J. Med. Chem.* **1998**, *41*, 102–108. (b) Morrison, C. F.; Elzein, E.; Jiang, B.; Ibrahim, P. N.; Marquart, T.; Palle, V.; Shenk, K. D.; Varkhedkar, V.; Maa, T.; Wu, L.; Wu, Y.; Zeng, D.; Fong, I.; Lustig, D.; Leung, K.; Zablocki, J. A. Structure-affinity relationships of 5′-aromatic ethers and 5′-aromatic sulfides as partial A_1 adenosine agonists, potential supraventricular anti-arrhythmic agents. *Bioorg. Med. Chem. Lett.* **2004**, *14*, 3793–3797.

(6) (a) Abdel-Hamid, M.; Novotny, M.; Hamza, H. Stability study of selected adenosine nucleosides using LC and LC/MS analyses. *J. Pharm. Biomed. Anal.* **2000**, *22*, 745–755. (b) Bennett, E. M.; Li, C.; Allan, P. W.; Parker, W. B.; Ealick, S. E. Structural basis for substrate specificity of Escherichia coli purine nucleoside phosphorylase. *J. Biol. Chem.* **2003**, *278*, 47110–47118.

(7) Hou, X.; Lee, H. W.; Tosh, D. K.; Zhao, L. X.; Jeong, L. S. Alternative and improved syntheses of highly potent and selective A_3 adenosine receptor agonists, Cl-IB-MECA and thio-Cl-IB-MECA. *Arch. Pharm. Res.* **2007**, *30*, 1205–1209.

(8) Franchetti, P.; Cappellacci, L.; Marchetti, S.; Trincavelli, L.; Martini, C.; Mazzoni, M. R.; Lucacchini, A.; Grifantini, M. 2′-*C*-Methyl analogues of selective adenosine receptor agonists: synthesis and binding studies. *J. Med. Chem.* **1998**, *41*, 1708–1715.

(9) Lohse, M. J.; Klotz, K.-N.; Schwabe, U.; Cristalli, G.; Vittori, S.; Grifantini, M. 2-Chloro-*N*6-cyclopentyladenosine: a highly selective agonist at A_1 adenosine receptors. *Naunyn-Schmiedeberg's Arch. Pharmacol.* **1988**, *337*, 687–689.

(10) Klotz, K.-N.; Lohse, M. J.; Schwabe, U.; Cristalli, G.; Vittori, S.; Grifantini, M. 2-Chloro-*N*6-[3H]cyclopentyladenosine ([3H]CCPA) - a high affinity agonist radioligand for A_1 adenosine receptors. *Naunyn-Schmiedeberg's Arch. Pharmacol.* **1989**, *340*, 679–683.

(11) Klotz, K.-N.; Hessling, J.; Hegler, J.; Owman, B.; Kull, B.; Fredholm, B. B.; Lohse, M. J. Comparative pharmacology of human adenosine receptor subtypes-characterization of stably transfected receptors in CHO cells. *Naunyn-Schmiedeberg's Arch. Pharmacol.* **1998**, *357*, 1–9.

(12) Klotz, K.-N.; Kachler, S.; Falgner, N.; Volpini, R.; Dal Ben, D.; Lambertucci, C.; Mishra, R. C.; Vittori, S.; Cristalli, G. [3H]HEMADO - a novel highly potent and selective radiolabeled agonist for A_3 adenosine receptors. *Eur. J. Pharmacol.* **2007**, *556*, 14–18.

(13) Palczewski, K.; Kumasaka, T.; Hori, T.; Behnke, C. A.; Motoshima, H.; Fox, B. A.; Le Trong, I.; Teller, D. C.; Okada, T.; Stenkamp, R. E.; Yamamoto, M.; Miyano, M. Crystal structure of rhodopsin: a G protein-coupled receptor. *Science* **2000**, *289*, 739–745.

(14) (a) Martinelli, A.; Tuccinardi, T. Molecular modeling of adenosine receptors: New results and trends. *Med. Res. Rev.* **2008**, *28*, 247–277. (b) Dal Ben, D.; Lambertucci, C.; Vittori, S.; Volpini, R.; Cristalli, G. GPCRs as therapeutic targets: a view on adenosine receptor structure and functions, and molecular modeling support. *J. Iran. Chem. Soc.* **2005**, *2*, 176–188. (c) Moro, S.; Deflorian, F.; Bacilieri, M.; Spalluto, G. Ligand-based homology modeling as attractive tool to inspect GPCR structural plasticity. *Curr. Pharm. Des.* **2006**, *12*, 2175–2185. (d) Costanzi, S.; Ivanov, A. A.; Tikhononva, I. G.; Jacobson, K. A. Structure and function of G protein-coupled receptors studied using sequence analysis, molecular modeling, and receptor engineering: Adenosine receptors. *Front. Drug Des. Discovery* **2007**, *3*, 63–79. (e) Jacobson, K. A.; Gao, Z.-G.; Liang, B. T. Neoceptors: Reengineering GPCRs to recognize tailored ligands. *Trends Pharmacol. Sci.* **2007**, *28*, 111–116. (f) Ballesteros, J. A.; Jensen, A. D.; Liapakis, G.; Rasmussen, S. G. F.; Shi, L.; Gether, U.; Javitch, J. A. Activation of the beta2-adrenergic receptor involves disruption of an ionic lock between the cytoplasmic ends of transmembrane segments 3 and 6. *J. Biol. Chem.* **2001**, *276*, 29171–29177.

(15) Lin, S. W.; Sakmar, T. P. Specific tryptophan UV-absorbance changes are probes of the transition of rhodopsin to its active state. *Biochemistry* **1996**, *35*, 11149–11159.
(16) (a) Cherezov, V.; Rosenbaum, D. M.; Hanson, M. A.; Rasmussen, S. G. F.; Thian, F. S.; Kobilka, T. S.; Choi, H.-J.; Kuhn, P.; Weis, W. I.; Kobilka, B. K.; Stevens, R. C. High-resolution crystal structure of an engineered human b2-adrenergic G protein-coupled receptor. *Science* **2007**, *318*, 1258–1265. (b) Rosenbaum, D. M.; Cherezov, V.; Hanson, M. A.; Rasmussen, S. G. F.; Thian, F. S.; Kobilka, T. S.; Choi, H.-J.; Yao, X. J.; Weis, W. I.; Stevens, R. C.; Kobilka, B. K. GPCR engineering yields highresolution structural insights into b2 adrenergic receptor function. *Science* **2007**, *318*, 1266–1273.
(17) Kim, S. K.; Gao, Z.-G.; Jeong, L. S.; Jacobson, K. A. Docking studies of agonists and antagonists suggest an activation pathway of the A_3 adenosine receptor. *J. Mol. Graph. Model.* **2006**, *25*, 562–577.
(18) Palaniappan, K. K.; Gao, Z.-G.; Ivanov, A. A.; Greaves, R.; Adachi, H.; Besada, P.; Kim, H. O.; Kim, A. Y.; Choe, S. A.; Jeong, L. S.; Jacobson, K. A. Probing the binding site of the A_1 adenosine receptor reengineered for orthogonal recognition by tailored nucleosides. *Biochemistry* **2007**, *46*, 7437–7448.
(19) Ivanov, A. A.; Palyulin, V. A.; Zefirov, N. S. Computer aided comparative analysis of the binding modes of the adenosine receptor agonists for all known subtypes of adenosine receptors. *J. Mol. Graph. Model.* **2007**, *25*, 740–754.
(20) Kim, J.; Wess, J.; van Rhee, A. M.; Schoneberg, T.; Jacobson, K. A. Site-directed mutagenesis identifies residues involved in ligand recognition in the human A_{2a} adenosine receptor. *J. Biol. Chem.* **1995**, *270*, 13987–13997.
(21) Olah, M. E.; Ren, H.; Ostrowski, J.; Jacobson, K. A.; Stiles, G. L. Cloning, expression, and characterization of the unique bovine A_1-adenosine receptor: Studies on the ligand binding site by site directed mutagenesis. *J. Biol. Chem.* **1992**, *267*, 10764–10770.
(22) Gao, Z.-G.; Jiang, Q.; Jacobson, K. A.; Ijzerman, A. P. Site-directed mutagenesis studies of human A_{2A} adenosine receptors. Involvement of Glu13 and His278 in ligand binding and sodium modulation. *Biochem. Pharmacol.* **2000**, *60*, 661–668.
(23) Gao, Z.-G.; Chen, A.; Barak, D.; Kim, S.-K.; Müller, C. E.; Jacobson, K. A. Identification by site-directed mutagenesis of residues involved in ligand recognition and activation of the human A_3 adenosine receptor. *J. Biol. Chem.* **2002**, *277*, 19056–19063.
(24) Rivkees, S. A.; Barbhaiya, H.; Ijzerman, A. P. Identification of the adenine binding site of the human A_1 adenosine receptor. *J. Biol. Chem.* **1999**, *274*, 3617–3621.
(25) Jiang, Q.; van Rhee, M.; Kim, J.; Yehle, S.; Wess, J.; Jacobson, K. A. Hydrophilic side chains in the third and seventh transmembrane helical domains of human A_{2A} adenosine receptors are required for ligand recognition. *Mol. Pharmacol.* **1996**, *50*, 512–521.
(26) Ruprecht, J. J.; Mielke, T.; Vogel, R.; Villa, C.; Schertler, G. F. X. Electron crystallography reveals the structure of metarhodopsin I. *EMBO J.* **2004**, *23*, 3609–3620.
(27) Shi, L.; Liapakis, G.; Xu, R.; Guarnieri, F.; Ballesteros, J. A.; Javitch, J. A. β_2 adrenergic receptor activation. Modulation of the proline kink in transmembrane 6 by a rotamer toggle switch. *J. Biol. Chem.* **2002**, *277*, 40989–40996.
(28) Gao, Z.-G.; Kim, S. K.; Gross, A. S.; Chen, A.; Blaustein, J. B.; Jacobson, K. A. Identification of essential residues involved in the allosteric modulation of the human A_3 adenosine receptor. *Mol. Pharmacol.* **2003**, *63*, 1021–1031.
(29) Dubuisson, D.; Dennis, S. G. The formalin test: a quantitative study of the analgesic effects of morphine, meperidine, and brain stem stimulation in rats and cats. *Pain* **1977**, *4*, 161–174.
(30) Maione, S.; De Novellis, V.; Cappellacci, L.; Palazzo, E.; Vita, D.; Luongo, L.; Stella, L.; Franchetti, P.; Marabase, I.; Rossi, F.; Grifantini, M. The antinociceptive effect of 2-chloro-2′-*C*-methyl-*N*6-cyclopentyladenosine (2′-Me-CCPA), a highly selective adenosine A_1 receptor agonist, in the rat. *Pain* **2007**, *131*, 281–292.
(31) *Molecular Operating Environment (MOE)*, version 2005.06; Chemical Computing Group, Inc.: Montreal, Canada, 2005.
(32) Huang, C. C.; Couch, G. S.; Pettersen, E. F.; Ferrin, T. E. Chimera: an extensible molecular modelling application constructed using standard components. *Pac. Symp. Biocomput.* **1996**, *1*, 724; http://www.cgl.ucsf.edu/chimera.
(33) Case, D. A.; Darden, T. A.; Cheatham, T. E., III; Simmerling, C. L.; Wang, J.; Duke, R. E.; Luo, R.; Merz, K. M.; Pearlman, D. A.; Crowley, M.; Walker, R. C.; Zhang, W.; Wang, B.; Hayik, S.; Roitberg, A.; Seabra, G.; Wong, K. F.; Paesani, F.; Wu, X.; Brozell, S.; Tsui, V.; Gohlke, H.; Yang, L.; Tan, C.; Mongan, J.; Hornak, V.; Cui, G.; Beroza, P.; Mathews, D. H.; Schafmeister, C.; Ross, W. S.; Kollman, P. A. *AMBER 9*; University of California, San Francisco: 2006.
(34) Cornell, W. D.; Cieplak, P.; Bayly, C. I.; Gould, I. R.; Merz, K. M. Jr.; Ferguson, D. M.; Spellmeyer, D. C.; Fox, T.; Caldwell, J. W.; Kollman, P. A. A second generation force field for the simulation of proteins, nucleic acids, and organic molecules. *J. Am. Chem. Soc.* **1995**, *117*, 5179–5197.
(35) Ballesteros, J. A.; Weinstein, H. Integrated methods for modelling G-protein coupled receptors. *Methods Neurosci.* **1996**, *25*, 366–428.
(36) (a) Olah, M. E.; Jacobson, K. A.; Stiles, G. L. Role of the second extracellular loop of adenosine receptors in agonist and antagonist binding. Analysis of chimeric A_1/A_3 adenosine receptors. *J. Biol. Chem.* **1994**, *269*, 24692–24698. (b) Kim, J.; Jiang, Q.; Glashofer, M.; Yehle, S.; Wess, J.; Jacobson, K. A. Glutamate residues in the second extracellular loop of the human A_{2a} adenosine receptor are required for ligand recognition. *Mol. Pharmacol.* **1996**, *49*, 683–691. (c) Rivkees, S. A.; Lasbury, M. E.; Barbhaiya, H. Identification of domains of the human A_1 adenosine receptor that are important for binding receptor subtype selective ligands using chimeric A_1/A_{2a} adenosine receptors. *J. Biol. Chem.* **1995**, *270*, 20485–20490.
(37) Bairoch, A.; Apweiler, R. The SWISS-PROT protein sequence database and its supplement TrEMBL in 2000. *Nucleic Acids Res.* **2000**, *28*, 45–48.
(38) Thompson, J. D.; Higgins, D. G.; Gibson, T. J. CLUSTAL W: Improving the sensitivity of progressive multiple sequence alignment through sequence weighting, position-specific gap penalties and weight matrix choice. *Nucleic Acids Res.* **1994**, *22*, 4673–4680.
(39) Fredriksson, R.; Lagerström, M. C.; Lundin, L. G.; Schiöth, H. B. The G-protein-coupled receptors in the human genome form five main families. Phylogenetic analysis, paralogon groups, and fingerprints. *Mol. Pharmacol.* **2003**, *63*, 1256–1272.
(40) McGuffin, L. J.; Bryson, K.; Jones, D. T. The PSIPRED protein structure prediction server. *Bioinformatics* **2000**, *16*, 404–405.
(41) Ryckaert, J.-P.; Ciccotti, G.; Berendsen, H. J. C. Numerical integration of the Cartesian equations of motion of a system with constraints: molecular dynamics of *n*-alkanes. *J. Comput. Phys.* **1977**, *23*, 327–341.
(42) Allen, F. H.; Bellard, S.; Brice, M. D.; Cartwright, B. A.; Doubleday, A.; Higgs, H.; Hummelink, T.; Hummelink-Peters, B. G.; Kennard, O.; Motherwell, W. D. S. The Cambridge Crystallographic Data Center: computer-based search, retrieval, analysis and display of information. *Acta Crystallogr., Sect. B: Struct. Sci.* **1979**, *35*, 2331–2339.
(43) (a) Halgren, T. A. Merck molecular force field. I. Basis, form, scope, parameterization, and performance of MMFF94. *J. Comput. Chem.* **1996**, *17*, 490–512. (b) Halgren, T. A. Merck molecular force field. II. MMFF 94 van der Waals and electrostatic parameters for intermolecular interactions. *J. Comput. Chem.* **1996**, *17*, 520–552. (c) Halgren, T. A. Merck molecular force field. III. Molecular geometries and vibrational parameters for intermolecular interactions. *J. Comput. Chem.* **1996**, *17*, 553–586. (d) Halgren, T. A. Merck molecular force field. IV. Conformational energies and geometries for MMFF94. *J. Comput. Chem.* **1996**, *17*, 587–615. (e) Halgren, T. A. Merck molecular force field. V. Extension of MMFF94 using experimental data, additional computational data, and empirical rules. *J. Comput. Chem.* **1996**, *17*, 616–641.
(44) Olah, M. E.; Stiles, G. L. The role of receptor structure in determining adenosine receptor activity. *Pharmacol. Ther.* **2000**, *85*, 55–75.
(45) Dawson, E. S.; Wells, J. N. Determination of amino acid residues that are accessible from the ligand binding crevice in the seventh transmembrane-spanning region of the human A_1 adenosine receptor. *Mol. Pharmacol.* **2001**, *59*, 1187–1195.
(46) Jacobson, K. A.; Gao, Z.-G.; Chen, A.; Barak, D.; Kim, S.-A.; Lee, K.; Link, A.; Van Rompaey, P. V.; Van Calenbergh, S.; Liang, B. T. Neoceptor concept based on molecular complementarity in GPCRs: a mutant adenosine A_3 receptor with selectivity enhanced affinity for amine-modified nucleosides. *J. Med. Chem.* **2001**, *44*, 4125–4136.
(47) De Lean, A.; Hancock, A. A.; Lefkowitz, R. J. Validation and statistical analysis of a computer modeling method for quantitative analysis of radioligands binding data for mixtures of pharmacological receptor subtypes. *Mol. Pharmacol.* **1982**, *21*, 5–16.
(48) Klotz, K.-N.; Cristalli, G.; Grifantini, M.; Vittori, S.; Lohse, M. J. Photoaffinity labeling of A_1-adenosine receptors. *J. Biol. Chem.* **1985**, *260*, 14659–14664.
(49) Saddi, G.; Abbott, F. V. The formalin test in the mouse: a parametric analysis of scoring properties. *Pain* **2000**, *89*, 53–63.
(50) Abbott, F. V.; Franklin, K. B.; Westbrook, R. F. The formalin test: scoring properties of the first and second phases of the pain response in rats. *Pain* **1995**, *60*, 91–102.

JM801456G